表 1　*EYS* 遺伝子変異をもつ患者の概要

症例	性別	年齢	遺伝形式	変異 1	変異 2	夜盲の自覚年齢	RP 診断時年齢	白内障混濁部位	白内障手術時年齢	よいほうの眼 視力	よいほうの眼 視野 I-4e	よいほうの眼 視野 V-4e
				短縮型変異ホモ接合体								
1	F	53	s	p.S1653Kfs*2	p.S1653Kfs*2	20	33	前嚢下白内障	50	0.2	測定不能	3
2	F	49	s	p.S1653Kfs*2	p.S1653Kfs*2	10	39	後嚢下白内障	50	1.0	3	8
3	F	43	ar	p.S1653Kfs*2	p.S1653Kfs*2	20	34	clear	—	0.02	測定不能	3
4	F	57	s	p.S1653Kfs*2	p.S1653Kfs*2	20	50	核白内障	58	0.04	2	5
5	M	38	s	p.S1653Kfs*2	p.S1653Kfs*2	10	37	前嚢下白内障	37	0.8	7	25
6	F	59	s	p.S1653Kfs*2	p.S1653Kfs*2	20	53	核白内障	57	0.1	2	5
7	M	50	s	p.S1653Kfs*2	p.S1653Kfs*2	20	40	核白内障	—	0.5	4	9
8	M	33	s	p.S1653Kfs*2	p.S1653Kfs*2	20	26	clear	—	1.0	7	8
9	F	45	ar	p.Y2935*	p.Y2935*	10	35	後嚢下白内障	45	0.4	2	7
10	F	58	s	p.Y2935*	p.Y2935*	10	18	核白内障	—	0.1	2	10
				短縮型変異を 2 つもつ複合ヘテロ接合体								
11	F	57	ar	p.S1653Kfs*2	p.N404Kfs*3	20	47	核白内障	—	0.3	3	8
12	F	47	ar	p.S1653Kfs*2	p.Y2935*	10	38	後嚢下白内障	47	0.04	測定不能	2
13	M	54	ar	p.Y2555*	p.Y2935*	10	39	核白内障	—	手動弁	測定不能	2
14	M	57	ar	p.S1653Kfs*2	p.Y2935*	20	33	核白内障	—	0.2	1	8
				短縮型変異とミスセンス変異による複合ヘテロ接合体								
15	F	67	s	p.S1653Kfs*2	p.G843E	20	41	核白内障	61	0.3	4	8
16	M	43	s	p.S1653Kfs*2	p.G843E	10	32	核白内障	—	0.7	5	10
17	F	69	ar	p.S1653Kfs*2	p.G843E	20	61	後嚢下白内障	67	0.5	4	8
18	M	51	s	p.S1653Kfs*2	p.G843E	10	48	後嚢下白内障	50	0.04	1	5
19	M	58	s	p.S2428*	p.G843E	10	42	核白内障	51	手動弁	測定不能	測定不能
20	F	54	ar	p.Y2935*	p.G843E	10	22	核白内障	—	手動弁	2	10
21	F	60	ar	p.S1653Kfs*2	p.G843E	20	44	clear	—	1.2	40	60
22	M	54	s	p.S1653Kfs*2	p.G2186E	20	44	後嚢下白内障	44	1.2	8	15
23	F	53	s	p.S1653Kfs*2	p.G843E	10	43	核白内障	48	1.2	5	15

2 つの創始者変異はそれぞれ，p.S1653Kfs*2 は 17 例，p.Y2935* は 6 例，の血縁関係のない複数の患者から同定された[3]。ar：常染色体劣性，s：孤発例。

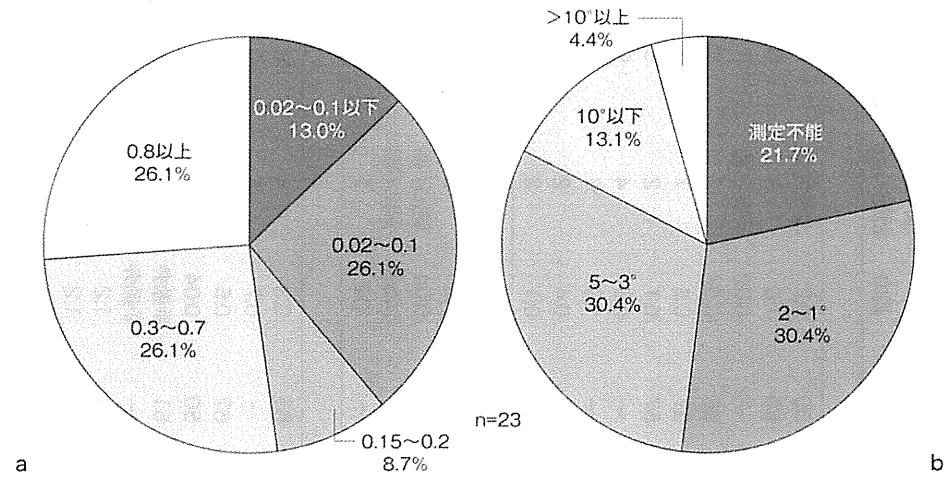

図 1　よいほうの眼における矯正視力の分布(a)と Goldmann 視野検査(Ⅰ-4 指標)(b)

考 按

今回の対象患者における年齢は，平均年齢 52.5±8.5 歳に代表される集団であり，成人期以降，特に 40 歳以降の中年期に進行を認める *EYS* 遺伝子変異の患者臨床像を理解するうえでは適した集団と考えられた[3]。夜盲の自覚年齢は，20 歳代で最も多く，これら *EYS* 遺伝子変異をもつ患者像の特徴として成人期まで自覚症状に乏しいことが観察された。これは患者の RP 診断時の平均年齢が 42.8 歳（33～61 歳）であったこととも矛盾しない結果であった。過去の報告によれば，日本人における定型 RP の 534 症例に基づく夜盲など自覚症状の発現時期は平均 26 歳[5]，定型 RP の 370 症例に基づく RP 診断の平均年齢は 35.1 歳との報告があり[6]，今回の *EYS* 遺伝子変異をもつ患者臨床像は，定型 RP を代表する遅発型かつ緩徐な経過を示すことが明らかとなった。

定型 RP における視力と視野に関する過去の報告において，早川ら[6]は 40～59 歳の RP 例における視力 0.1 以下の眼は 38%とされている。実際，今回の対象群（平均年齢 52.5 歳）においても，視力 0.1 以下の眼は 9 例（39.1%）であり，定型 RP にみられる緩徐な進行を示す結果であった。また視野については，30 歳代の症例 5，症例 8 の 2 例に着目した場合に，ともに視力は 0.8 以上と良好ではあったが，Ⅰ-4e 指標の半径に基づく求心性視野狭窄はともに 7° と大きく進行を認めており（表 1），視野障害については 20～30 歳で視力低下に先行して進行する傾向があることが推測された。視野狭窄については，平均年齢 52.5 歳においてⅠ-4e 指標の半径に基づく求心性視野狭窄 5° 以下の群が 19 例（82.6%）であり，視力が比較的に維持されていても，中年期以降における日常生活上の困難が強く予想された。また，視力 0.1 以下の眼（9 例，43～59 歳）は，全例が求心性視野狭窄 3° 未満に含まれていた。以上から，視力 0.1 以下への視力低下は，白内障による視力低下を除外したうえで，RP の進行病期における予後不良の因子となりうることが推測された。

今回の対象 23 例のうち 20 例（86.9%）が白内障診断を受けており，13 例（56.5%）で平均年齢 51.1 歳（38～67 歳）における白内障手術既往があった。これらの結果より，白内障の進行時期については中年期（40～60 歳ごろ）に多いことが推測され，健常者と比較してより早期に発症，進行することが示唆された。過去の海外の報告においても同様に，*EYS* 遺伝子変異をもつ患者における白内障が高頻度であること，若年の症例で嚢下白内障が観察されたことが報告されている[7]。

日本人 arRP において，比較的高頻度にみられる *EYS* 遺伝子変異は，夜盲に始まり成人期以降の緩徐な視野狭窄の進行と視力低下を認める，典型的な遅発型の RP 臨床像を呈する可能性がある。また，高頻度にみられる併発白内障の管理には留意する必要が推測された。今後，遺伝子診断，

そして遺伝カウンセリングにおいて，これら*EYS*遺伝子変異による臨床像を理解することは有用と考えられた。

利益相反：該当なし

文献

1) Abd El-Aziz MM, Barragan I, O'Driscoll CA et al：*EYS*, encoding an ortholog of *Drosophila spacemaker*, is mutated in autosomal recessive retinitis pigmentosa. Nat Genet **40**：1285-1287, 2008
2) Collin RW, Littink KW, Klevering BJ et al：Identification of a 2 Mb human ortholog of *Drosophila eyes shut/spacemaker* that is mutated in patients with retinitis pigmentosa. Am J Hum Genet **83**：594-603, 2008
3) Iwanami M, Oshikawa M, Nishida T et al：High prevalence of mutations in the *EYS* gene in Japanese patients with autosomal recessive retinitis pigmentosa. Invest Ophthalmol Vis Sci **53**：1033-1040, 2012
4) Hosono K, Ishigami C, Takahashi M et al：Two novel mutations in the *EYS* gene are possible major causes of autosomal recessive retinitis pigmentosa in the Japanese population. PLoS One **7**：e31036 2012
5) Tsujikawa M, Wada Y, Sukegawa M et al：Age at onset curves of retinitis pigmentosa. Arch Ophthalmol **126**：337-340, 2008
6) 早川むつ子・藤木慶子・村松美代・他：原発性定型網膜色素変性の遺伝的異質性と予後に関する18施設調査．臨眼 **46**：1025-1029, 1992
7) Audo I, Sahel JA, Mohand-Saïd S et al：*EYS* is a major gene for rod-cone dystrophies in France. Hum Mutat **31**：E1406-E1435, 2010

V. 参考資料

High Prevalence of Mutations in the *EYS* Gene in Japanese Patients with Autosomal Recessive Retinitis Pigmentosa

Masaki Iwanami,[1,2] *Mio Oshikawa,*[2] *Tomomi Nishida,*[1] *Satoshi Nakadomari,*[1] *and Seishi Kato*[2]

Purpose. To screen for disease-causing mutations in the Eyes shut homolog (*EYS*) gene in Japanese patients with retinitis pigmentosa (RP).

Methods. Blood samples were obtained from 68 RP patients and 68 controls. Genomic DNA was extracted from the blood samples and used for screening of mutations in the coding exons by direct sequencing. Each patient underwent a detailed clinical examination.

Results. Nine nucleotide sequence variations causing amino acid changes were observed in homozygous or heterozygous alleles in 26 patients but not in 68 controls. Seven truncating mutations were found in 21 (32.8%) of 64 patients with nonsyndromic RP composed of 23 autosomal recessive RP (arRP) and 41 sporadic cases. The most abundant mutation was p.S1653Kfs*2, which was generated by a single adenine insertion into exon 26 (c.4957dupA) and was carried by 15 patients. The mutation p.Y2935*, produced by a single nucleotide substitution (c.8805C>A) in the last exon, was carried by five patients. These two truncating mutations were probably founder mutations because each was carried by the particular haplotype. The patients with homozygous or compound heterozygous truncating mutations showed a severe decline in visual acuity, whereas those with a single truncating mutation showed a mild decline.

Conclusions. One-third of Japanese patients with nonsyndromic arRP carried probable pathogenic mutations in the *EYS* gene, including two founder mutations. Because the genotype was correlated with the phenotype, genotyping in the *EYS* gene could be a valuable tool for predicting long-term prognoses of Japanese patients with arRP and thus could be useful for genetic counseling and future gene therapy. (*Invest Ophthalmol Vis Sci.* 2012;53:1033–1040) DOI:10.1167/iovs.11-9048

Retinitis pigmentosa (RP) is the most common genetic disorder in inherited retinal dystrophy. It has a prevalence of approximately 1 in 4000 persons worldwide.[1] In Japan, RP was the major cause of visual impairment among persons who entered 29 rehabilitation centers during the past 20 years, accounting for 25.0% (2001) and 15.8% (2006) of these cases.[2] RP is characterized by progressive visual loss caused by degenerative abnormalities of retinal photoreceptors. In the early stages, rod photoreceptor function is predominantly impaired, leading to defective dark adaptation, night blindness, and constriction of the visual field, followed by impairment of visual acuity from the loss of cone photoreceptor cells and eventually complete blindness.[1]

RP is genetically heterogeneous; it is transmitted as an autosomal dominant (ad), autosomal recessive (ar), or X-linked recessive disorder. To date more than 42 causative genes and seven loci have been identified (RetNet [http://www.sph.uth.tmc.edu/RetNet]), which is estimated to account for approximately 50% of all cases.[3] Thirty-two genes have been identified for the autosomal recessive form of RP (arRP). Mutation in each gene is observed in 1% to 2% of arRP cases,[4] with the exceptions of ATP-binding cassette, sub-family A, member 4 (*ABCA4*) and Usher syndrome type2A (*USH2A*) genes, mutations of which are observed in 5.6% and 7.0% of arRP patients, respectively.[5,6] Recent reports have suggested a global involvement of *EYS*, with the prevalence in different populations of persons with arRP (e.g., Spanish, French, Israeli) ranging from approximately 5% to 15%.[7–13] In Japan, large-scale mutation screening of *ABCA4*,[14] rhodopsin,[15] and 30 RP-causing genes[16] have been performed on arRP patients, but no major gene responsible for RP has been identified.

EYS (Online Mendelian Inheritance in Man no. 612424) is the largest gene known to be expressed in the human eye, spanning more than 2 Mb within the *RP25* locus (6q12).[7,8] The human EYS protein is a homolog of the *Drosophila* eyes shut/spacemaker (eys) protein, which is an extracellular matrix protein essential for photoreceptor development and morphology of the insect eye.[17,18] The longest isoform of *EYS* encodes a protein of 3165 amino acids, containing a signal peptide, 28 EGF-like domains, and 5 laminin A G-like domains (LamG).[7,8] All types of mutations have been reported in *EYS*: insertion, deletion, nonsense or missense substitution, and splice site mutation.[7–13] Most are truncating mutations, leading to premature truncation codons (PTCs). Some missense mutations were also identified by segregation studies and found in combination with a truncating mutation as probable causative mutations.[9–13,19] *EYS* is expressed in the retina, and the EYS protein is localized to outer segments of photoreceptor cells. Considering the evolutionary data and the function of the *Drosophila* homolog eys, EYS is likely to play a role in the modeling of retinal architecture.[17,18]

In this study, we screened 68 Japanese RP patients who visited the low-vision clinic at our center to search for RP-associated mutations in the *EYS* gene. As a result, we found that *EYS* is a major causative gene of nonsyndromic arRP in the Japanese population. The genotype-phenotype correlation was examined to serve as a prognostic indicator.

From the [1]Department of Ophthalmology, Hospital, and [2]Department of Rehabilitation Engineering, Research Institute, National Rehabilitation Center for Persons with Disabilities, Tokorozawa, Japan.

Submitted for publication November 10, 2011; revised December 12, 2011; accepted January 3, 2012.

Disclosure: **M. Iwanami**, None; **M. Oshikawa**, None; **T. Nishida**, None; **S. Nakadomari**, None; **S. Kato**, None

Corresponding author: Masaki Iwanami, Department of Ophthalmology, Hospital, National Rehabilitation Center for Persons with Disabilities, 4-1 Namiki, Tokorozawa, Saitama 359-8555, Japan; miwanami1@gmail.com.

METHODS

Subjects

We studied 68 unrelated RP patients who visited the low-vision clinic at our center, as previously reported.[15,20] RP subjects were selected on the basis of clinical findings, patient history, and family history. Of these 68 patients, 4 were diagnosed as having adRP and 64 as having nonsyndromic arRP; the latter group consisted of 23 pedigrees with a recessive mode of inheritance (arRP) and 41 sporadic cases. Sixty-eight controls were recruited from among students at a college affiliated with our center and members of our staff of the center, all of whom declared having neither a personal history nor a family history of night blindness or unexplained visual loss. The study was approved by the institutional review board of the National Rehabilitation Center for Persons with Disabilities and was conducted in accordance with the Declaration of Helsinki. Informed consent was obtained from all subjects in this study.

Genetic Analysis

Genomic DNA was isolated from venous blood of the subjects using a DNA purification kit (Puregene; Gentra Systems, Minneapolis, MN). An additional 100 control DNA samples isolated from B-lymphoblast cell lines derived from unrelated healthy Japanese volunteers were obtained from the Health Science Research Resources Bank (Osaka, Japan). The genomic sequence of the *EYS* locus (NT_007299.13) and mRNA sequence (NM_001142800.1) were retrieved from the National Center for Biotechnology Information. Nucleotide A of the initiation codon of *EYS* was defined as position 1. The intronic primer sequences of 40 coding exons of the *EYS* gene for polymerase chain reaction (PCR) amplification are listed in Supplementary Table S1 (http://www.iovs.org/lookup/suppl/doi:10.1167/iovs.11-9048/-/DCSupplemental). Two hundred nanograms of genomic DNA were amplified with *Taq* polymerase (TaKaRa PrimeSTAR; Takara Bio Inc., Shiga, Japan), and mutation analysis was performed by direct sequencing of purified PCR products (BigDye Terminator Cycle Sequencing Kit; Applied Biosystems, Foster City, CA). The sequence primers are listed in Supplementary Table S2 (http://www.iovs.org/lookup/suppl/doi:10.1167/iovs.11-9048/-/DCSupplemental). Sequencing reaction products were run on an automated capillary sequencer (3130xl Genetic Analyzer; Applied Biosystems). The sequence variations were designated in accordance with the Human Genome Variation Society recommendations (http://www.hgvs.org/).

Haplotype Analysis

Haplotypes were estimated from unphased genotypes using Clark's algorithm[21] and the expectation-maximization (EM) algorithm.[22] The Arlequin program (Schneider, Roessli, Excoffier, Arlequin version 2.000: a software package for population genetics data analysis; Geneva, Switzerland) was used for the analysis using the EM algorithm. The haplotype block in the *EYS* locus was estimated on the basis of LD plot analysis using HapMap (http://hapmap.ncbi.nlm.nih.gov/cgi-perl/gbrowse/hapmap27_B36/).

Clinical Evaluation

A complete ophthalmic examination was performed, including refraction, visual acuity, visual field, biomicroscopic slit lamp examination, electroretinography (ERG), and funduscopy. Best-corrected visual acuity was measured in each eye with a Landolt chart, and the decimal values were converted to the logarithm of the minimal angle of resolution (logMAR) units. The visual field was assessed by Goldman kinetic perimetry (V-4e, I-4e, and I-2e targets). The clinical diagnosis was based on visual acuity, visual field, fundus photographs, and ERG findings. ERG recordings were performed in accordance with the guidelines provided by the International Society for Clinical Electrophysiology of Vision, using a monopolar contact lens electrode. Basic retinal imaging was performed using color fundus photographs, and an

TABLE 1. Mutations Causing Amino Acid Changes Found in the *EYS* Gene of Japanese Patients with Retinitis Pigmentosa

Marker	Exon	Nucleotide Change	Amino Acid Change	Domain*	Type	SNP ID	RP†	Control‡	Reference
SV04	8	c.1211dupA	p.Asn404Lysfs*3	EGF	Frameshift	—	1	0	11
SV09	10	c.1485_1493delGGTTATTGAinsCGAAAAG	p.Val495Glufs*13	EGF	Frameshift	—	1	0	Novel
SV25	16	c.2528G>A	p.Gly843Glu	EGF	Missense	rs74419361	11	2	dbSNP§
SV38	23	c.3489T>A	p.Asn1163Lys	EGF	Missense	rs150951106	1	0	9,12
SV42	25	c.3809T>G	p.Val1270Gly	EGF	Missense	—	1	0	Novel
SV59	26	c.4957dupA	p.Ser1653Lysfs*2	Close to coiled-coil	Frameshift	—	22	0	Novel
SV77	35	c.7028_7029delTGinsATCGT	p.Leu2343Hisfs*105	EGF	Frameshift	—	1	0	Novel
SV80	37	c.7283C>A	p.Ser2428*	LamG	Nonsense	—	1	0	Novel
SV81	39	c.7665_7666delCA	p.Tyr2555*	LamG	Nonsense	—	1	0	Novel, 10‖
SV83	43	c.8805C>A	p.Tyr2935*	EGF	Nonsense	—	6	0	Novel

* According to Abd El-Aziz et al.[7] and Collin et al.[8]

† The number of chromosomes found in 136 chromosomes of 68 patients with retinitis pigmentosa.

‡ The number of chromosomes found in 136 chromosomes of 68 controls.

§ Short genetic variations database in the National Center for Biotechnology Information.

‖ The same amino acid change but different nucleotide change.

optical coherence tomography (OCT) device (Spectralis; Heidelberg Engineering, Heidelberg, Germany) was also used in some patients.

Results

Sequence Variations

Supplementary Table S3 (http://www.iovs.org/lookup/suppl/doi:10.1167/iovs.11-9048/-/DCSupplemental) shows the nucleotide sequence variations in the *EYS* gene found in a total of 136 chromosomes from 68 RP patients, of whom 64 had nonsyndromic arRP (23 arRP and 41 sporadic) and 4 had adRP. We identified 83 nucleotide sequence variations that correspond to markers SV01 to SV83 in Supplementary Table S3 (http://www.iovs.org/lookup/suppl/doi:10.1167/iovs.11-9048/-/DCSupplemental), consisted of 66 single nucleotide substitutions and 16 insertion/deletion variations; 16 of these variations were novel. The 10 variations causing amino acid changes are listed in Table 1; they consisted of 3 missense variations (1 was novel) and 7 truncating mutations (6 were novel). SV25 (p.G843E) was included in the list in spite of a probable rare single nucleotide polymorphism (SNP) found in controls because it was unexpectedly abundant in RP patients compared with controls. Truncating mutations were produced by substitution (SV80, SV83), insertion (SV04, SV59), replacement (SV09, SV77), or deletion (SV81). Interestingly, SV59 (p.S1653Kfs*2) and SV83 (p.Y2935*) were found in multiple patients, as was p.G843E.

The amino acid sequence changes were observed in homozygous or heterozygous alleles in 26 of the RP patients, including 11 arRP and 14 sporadic cases, as shown in Table 2, but not in the 68 controls, with the exception of p.G843E, which was carried by 2 controls. Seven truncating mutations were found in 21 (32.8%) of the 64 patients with nonsyndromic arRP. Three missense variations were observed in 12 patients. The patients were classified into 5 groups on the basis of allele types: group A consisted of patients with homozygous truncating mutations, group B of patients with probable compound heterozygous truncating mutations, group C of patients with heterozygous truncating and missense mutations, group D of patients with single heterozygous truncating mutations, and group E of patients with missense mutations.

Truncating Mutations

Seven truncating mutations were found in 22 out of 68 RP patients (Table 2). The most abundant one was p.S1653Kfs*2, which was generated by a single adenine insertion into exon 26 (c.4957dupA), and was carried by 15 (15/64 = 23.4%) of the 64 non-syndromic arRP patients and 1 adRP patient (RP37). As shown in Table 2, 7 patients were homozygous (group A), 4 were probable compound heterozygous (group B), and 11

Table 2. Retinitis Pigmentosa Patients Carrying *EYS* Mutations

No.	Patient	Sex	Age (y)	Inheritance	Mutation 1	Mutation 2
Group A, homozygous truncating mutations						
1	RP37*	F	43	ad	p.S1653Kfs*2	p.S1653Kfs*2
2	RP63†	M	35	ar	p.S1653Kfs*2	p.S1653Kfs*2
3	RP04	F	53	s	p.S1653Kfs*2	p.S1653Kfs*2
4	RP12	F	49	s	p.S1653Kfs*2	p.S1653Kfs*2
5	RP38	F	57	s	p.S1653Kfs*2	p.S1653Kfs*2
6	RP57	M	52	s	p.S1653Kfs*2	p.S1653Kfs*2
7	RP49‡	F	45	ar	p.Y2935*	p.Y2935*
Group B, probable compound heterozygous truncating mutations						
8	RP16	F	57	ar	p.S1653Kfs*2	p.N404Kfs*3
9	RP44‡	F	47	ar	p.S1653Kfs*2	p.Y2935*
10	RP54	M	56	s	p.V495Efs*13	p.L2343Hfs*105
11	RP29	M	54	s	p.Y2935*	p.Y2555*
Group C, heterozygous truncating and missense mutations						
12	RP43	F	69	ar	p.S1653Kfs*2	p.G843E
13	RP62	M	63	ar	p.S1653Kfs*2	p.G843E
14	RP08	F	67	s	p.S1653Kfs*2	p.G843E
15	RP28	M	43	s	p.S1653Kfs*2	p.G843E
16	RP55	M	51	s	p.S1653Kfs*2	p.G843E
17	RP50	M	58	s	p.S2428*	p.G843E
Group D, single heterozygous truncating mutation						
18	RP03†	F	56	ar	p.S1653Kfs*2	—
19	RP61	F	62	s	p.S1653Kfs*2	—
20	RP68	M	54	s	p.S1653Kfs*2	—
21	RP26	F	28	ar	p.Y2935*	—
22	RP45	M	64	ar	p.Y2935*	—
Group E, missense mutation						
7	RP49‡	F	45	ar	p.G843E	p.G843E
23	RP21	M	33	ar	p.G843E	—
9	RP44‡	F	47	ar	p.G843E	—
24	RP66	M	71	s	p.G843E	—
25	RP10	F	50	ar	p.N1163K	—
26	RP14	F	54	s	p.V1270G	—

ar, autosomal recessive; ad, autosomal dominant; s, sporadic.

* Probably consanguineous marriage.

† Consanguineous marriage.

‡ Having both truncating and missense mutations.

were heterozygous (group C and D). Probable compound heterozygous mutations in combination with p.S1653Kfs*2 were identified: p.N404Kfs*3 for RP16, p.Y2935* for RP44, and p.G843E for 5 patients. RP37 in the adRP panel had homozygous p.S1653Kfs*2 alleles, suggesting the possibility of arRP. The other 3 adRP patients had no mutation in the *EYS* gene.

Mutation p.Y2935* in the last exon was produced by a single nucleotide substitution (c.8805C>A), which was carried by 5 patients. RP49 was homozygous for this mutation. RP44 and RP29 were probable compound heterozygous in combination with p.S1653Kfs*2 and p.Y2555*, respectively. RP26 and RP45 were single heterozygous.

RP54 carried double heterozygous mutations, both of which were produced by replacement: c.1485_1493 delGGTTATTGAinsCGAAAAG (p.V495Efs*13) and c.7028_7029delTGinsATCGT (p.L2343Hfs*105). The remaining single truncating mutations (p.N404Kfs*3, p.S2428*, p.Y2555*) were combined with one of three abundant mutations as described above. The mutation p.N404Kfs*3 (C.1211dupA) was previously reported in a Moroccan Jewish patient.[11] p.Y2555* was reported in Caucasian patient,[10] but the genotype (c.7665C>G) was different from that (c.7665_7666delCA) observed in our case.

Missense Mutations

Of 3 missense mutations, p.G843E in exon 16 was carried by 10 patients, and the allele frequency was 8.1% in RP patients. This substitution has already been annotated as SNP (c.2528G>A, rs74419361) with an allele frequency of 1.3% in the 1000 genomes (http://www.1000genomes.org/). In fact, this substitution was detected in 2 of the 68 controls and 1 of the samples from another 100 Japanese controls. RP49 was homozygous for p.G843E as well as for p.Y2935* and thus carried 2 different homozygous mutations. RP44 carrying combined truncating mutations also had heterozygous p.G843E. Six patients carrying p.G843E were heterozygous in combination with 2 truncating mutations (group C), and 2 were single heterozygous (group E). The single heterozygous mutations p.N1163K and p.V1270G were detected in RP10 and RP14, respectively.

Haplotype Analysis

The truncating mutations p.S1653Kfs*2 and p.Y2935* were carried by multiple patients (16 and 5, respectively), suggesting that these mutations are probably founder mutations rather than recurrent mutations. If the mutation is attributed to a founder effect, the mutation should exist in a particular haplotype. To examine this possibility, the haplotype structures around these mutations were estimated using SNPs obtained from 68 patients and 68 controls. First, the region of the haplotype block containing each mutation was estimated on the basis of LD plot analysis using HapMap. The RP patient-derived SNPs found within each haplotype block were used to estimate the haplotype of this region. Tables 3 and 4 show the haplotype structures, suggesting that each mutation exists in a particular haplotype: HBA03 for SV59 (p.S1653Kfs*2) and HBB01 for SV83 (p.Y2935*). HBA03 is a minor haplotype with a frequency of only 8.1% in the controls, while HBB01 is a major haplotype with a frequency of 57.4% in the controls. The results strongly support that these two mutations are probable founder mutations. In addition, the haplotype structure around SV25 (p.G843E) was estimated, and this variation was confirmed to be a SNP characterizing a haplotype HBC06 as shown in Table 5.

Clinical Features

Clinical and functional findings in 26 patients harboring the *EYS* mutations are summarized in Supplementary Table S4, http://

TABLE 3. Haplotypes of the Region around SV59 (p.S1653Kfs*2)

Haplotype Name	Sequence Variation Marker													Patients		Controls	
	SV46	SV48	SV49	SV50	SV51	SV52	SV53	SV54	SV55	SV56	SV57	SV59	SV60	SV61	Chromosomes	Frequency	Chromosomes	Frequency
HBA01	C	C	A	C	C	A	C	T	C	A	G	—	A	C	54	0.397	82	0.603
HBA02	C	C	A	C	C	A	T	T	C	A	G	—	A	C	41	0.301	34	0.250
HBA03	G	T	G	G	T	G	C	C	T	G	A	—	A	G	12	0.088	11	0.081
HBA03m	G	T	G	G	T	G	C	C	T	G	A	insA	A	G	22	0.162	0	0.000
HBA04	C	C	A	C	C	A	C	T	C	A	G	—	C	C	7	0.052	7	0.051
HBA05	C	C	A	C	C	A	C	C	T	G	A	—	A	G	0	0.000	2	0.015
Total															136	1	136	1

TABLE 4. Haplotypes of the Region around SV81 (p.Tyr2555*) and SV83 (p.Tyr2935*)

Haplotype Name	Sequence Variation Marker			Patients		Controls	
	SV79	SV82 (SV81)	SV83	Chromosomes	Frequency	Chromosomes	Frequency
HBB01	A	A	C	52	0.382	78	0.574
HBB01m	A	A	A	7	0.052	0	0
HBB02	G	A	C	42	0.309	31	0.228
HBB02m	G	del	C	1	0.007	0	0
HBB03	A	T	C	34	0.25	27	0.198
Total				136	1	136	1

www.iovs.org/lookup/suppl/doi:10.1167/iovs.11-9048/-/DCSupplemental. The patients' age ranged from 28 to 71 years (average 52) when genomic testing was performed. These patients showed typical RP symptoms such as night blindness and progressive constriction of visual fields. Both myopic and hyperopic refractive errors were present. Cataracts were seen at a relatively young age. Fifteen patients had a cataract surgery, and their ages at the time of surgery ranged from 31 to 67 (average 50). Fundus appearance was typical for RP, including attenuation of the retinal arteries and bone spicule pigment deposits in the mid-periphery of the retina. Pallor of the optic discs was observed in patients at the end stage. Electroretinography responses were non-recordable in all patients with the *EYS* mutations in this study.

Segregation Analysis

A segregation study was performed for the family of RP38 with the probable founder mutation p.S1653Kfs*2, and the results showed that the disease phenotype segregated the subjects (Fig. 1). The OCT images of a horizontal section including the macular and peripheral region demonstrated a reduction of retinal thickness in RP38 (II-1) due to the loss of sensory retinal tissue (Fig. 1C). The mother (I-2, age 91) and the sibling (II-4, age 58) were carriers of p.S1653Kfs*2 without manifestation of the RP phenotype. The fundus images of the sibling and mother were normal (Figs. 1D, 1E), although the mother had the cataract. The OCT image of the sibling clearly showed the normal retinal structure (Fig. 1D).

Genotype-Phenotype Correlation

To characterize the genotype-phenotype correlation, the clinical features were compared among the different groups (groups A-D). Fifteen patients revisited our center for clinical follow-up, so that the time course data of the visual acuity and visual field were available. To examine the relationship between these clinical features and genotype, the time course of the visual acuity of the patients was plotted in Figure 2 using the data available for 5 patients from group A, 3 from group B, 5 from group C, and 2 from group D. During the clinical follow-up period (2–12 years; average, 7.3 years), patients in groups A and B, who carried homozygous or compound heterozygous truncating mutations, showed a severe decline in visual acuity, except RP12 and RP49 (Fig. 2A). Similarly, a severe decline was observed in the visual field of all these patients except RP37 (Supplementary Fig. S1A, http://www.iovs.org/lookup/suppl/doi:10.1167/iovs.11-9048/-/DCSupplemental). In contrast, patients in groups C and D, who carried a heterozygous truncating mutation, showed a mild decline in visual acuity and visual field (Fig. 2B; Supplementary Fig. S1B, http://www.iovs.org/lookup/suppl/doi:10.1167/iovs.11-9048/-/DCSupplemental). RP50 showed severe loss of visual acuity and visual field in his 50s, whereas RP08 and RP43 showed residual functions in central vision and visual field at ages 69 and 76, respectively.

The phenotypes characterized by the time course of the visual acuity and visual field were confirmed by the fundus and OCT images of patients in each group. For example, RP04, with a severe decline of visual field in group A, showed the end stage of severe retinal thinning and foveal atrophy at age 60, with clumping structures that seemed to be composed of the proliferating retinal pigment epithelial cells (Fig. 3A). RP49, with a moderate decline of visual field in group A, showed moderate loss of sensory retinal tissue (Fig. 3B). RP43 in group C and RP68 in group D showed preserved sensory retinal tissue with the junction line between the inner and outer segments of photoreceptor cells in the macular region (Figs. 3C, 3D), suggesting the weaker pathogenicity of a single heterozygous truncating mutation.

DISCUSSION

We found that one-third of Japanese patients with nonsyndromic arRP carried probable pathogenic mutations in the *EYS* gene. This prevalence is higher than the prevalences reported in other populations: 11% in British and Chinese,[10] 12% in French,[9] 5% in Dutch and Canadian,[12] 7% in Israeli,[11] and 15.9% in Spanish.[13] This high prevalence can be attributed to the existence of two major variants, p.S1653Kfs*2 and

TABLE 5. Haplotypes of the Region around SV25 (p.G843E)

Haplotype Name	Sequence Variation Marker						Patients		Controls	
	SV23	SV24	SV25	SV26	SV27	SV28	Chromosomes	Frequency	Chromosomes	Frequency
HBC01	T	C	G	T	A	A	50	0.368	57	0.419
HBC02	T	G	G	C	A	C	43	0.316	44	0.324
HBC03	C	C	G	T	A	A	26	0.191	21	0.154
HBC04	T	G	G	C	G	C	6	0.044	7	0.051
HBC05	C	G	G	C	A	C	0	0.000	5	0.037
HBC06	T	G	A	C	A	C	11	0.081	2	0.015
Total							136	1	136	1

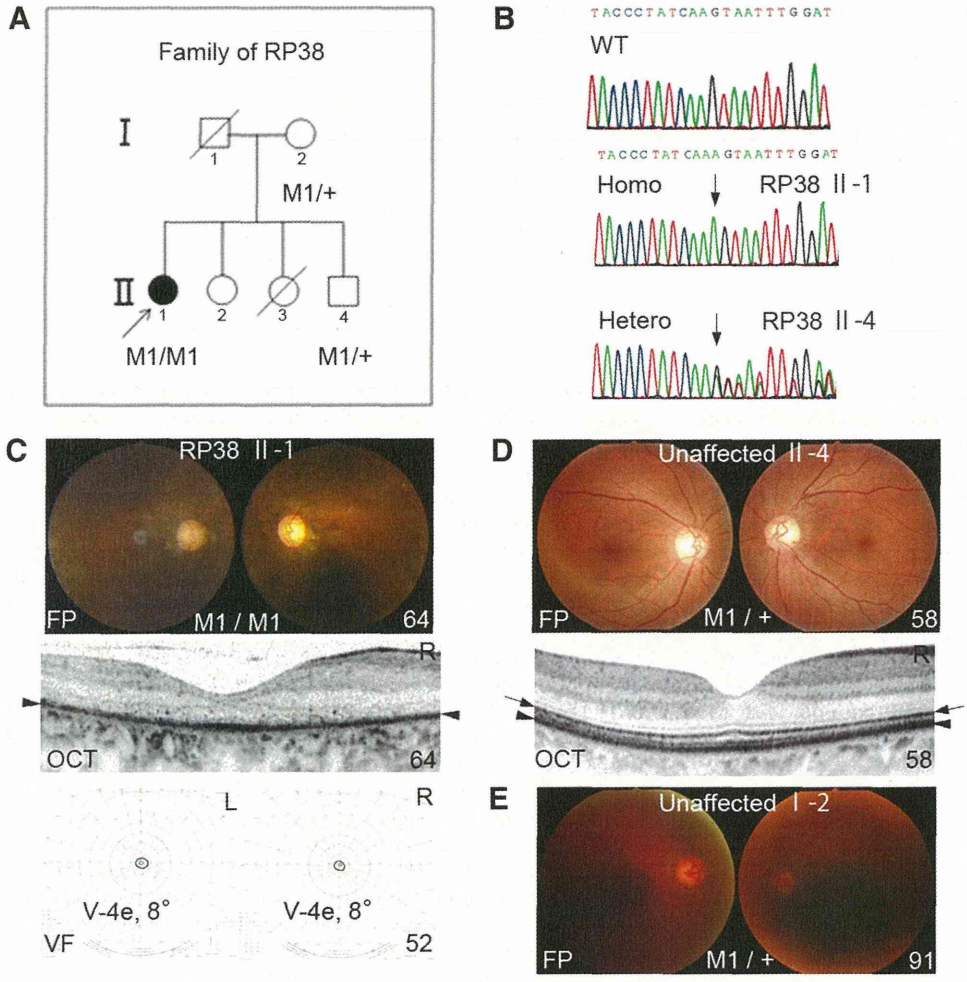

FIGURE 1. Segregation study for the family of RP38. (**A**) Pedigree of the family of RP38, who carried p.S1653Kfs*2 (M1). *Arrow*: Proband. M1/M1 represents a homozygous mutant, whereas M1/+ indicates a heterozygous carrier. (**B**) Mutation found in the RP38 family. c.4957dupA causes p.S1653Kfs*2. The proband (II-1) has homozygous mutations, and the unaffected sibling (II-4) has a heterozygous allele. Clinical features of the proband II-1 (**C**), the affected sibling II-4 (**D**), and the unaffected mother I-2 (**E**) were shown. FP, fundus photograph; OCT, optical coherence tomography; VF, visual field; L, left; R, right. The *number* in each panel indicates the age of the patient when the examination was performed. In the OCT panel, an *arrow* indicates the junction between the inner and outer segments of photoreceptors, and an *arrowhead* indicates an RPE complex.

p.Y2935*, which are probably founder mutations because each was carried by the particular haplotype. The discovery of these founder mutations will greatly simplify diagnostic genetic screening in Japanese arRP patients, and these mutations will become a potential target for gene therapy. Similar founder mutations in the *EYS* gene have been reported in other ethnic populations: p.T135Lfs*26 in Moroccan Jewish,[11] p.H2740Yfs*28 in Iraqi Jewish,[11] and p.Y3156* in Dutch.[8] Further examination is necessary to reveal the origin of these population-specific founder mutations.

The genotypes of group A (homozygous truncating mutations) and group B (probable compound heterozygous truncating mutations), shown in Table 2, meet the requirement for an autosomal recessive mode of inheritance, suggesting that all truncating mutations in these groups are pathogenic. In fact, most patients in these groups showed a severe decline in visual acuity. Since the mRNA transcribed from the *EYS* gene containing these truncating mutations has a PTC, the transcripts should be degraded by the nonsense-mediated decay (NMD) mechanism,[25] leading to the loss of the EYS protein. Alternatively, the truncating mutations may produce a truncated EYS protein lacking the C-terminal region, which has no or little of the function of EYS. The patients in groups C and D had a single truncating mutation (p.S1653Kfs*2 or p.Y2935*). Most of these patients showed a mild decline in visual acuity. Thus, we could predict the prognosis of the patient by examining whether the patient had homozygous truncating mutations or a single heterozygous truncating mutation. Considering the non-adRP mode of inheritance, each patient with a single truncating mutation should have had another mutation allele.

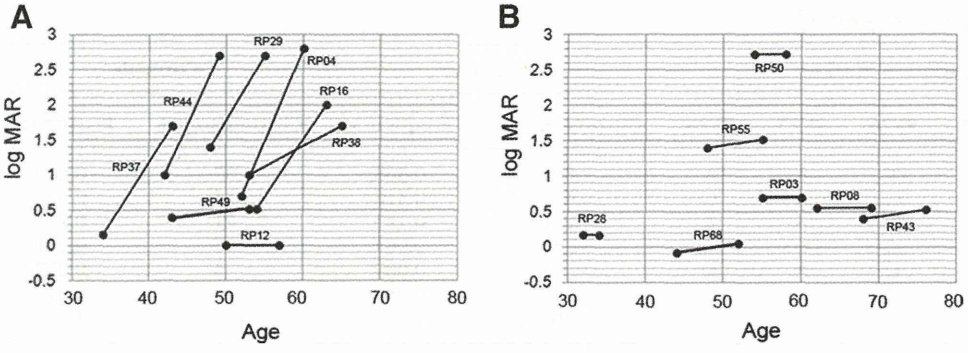

FIGURE 2. The time course of visual acuity score in the right eye. (**A**) Patients carrying homozygous truncating mutations or probable compound heterozygous truncating mutations. (**B**) Patients carrying a heterozygous truncating mutation. Visual acuity was measured with a Landolt chart, and the decimal values were converted to the logMAR units. 2.7 logMAR and 2.8 logMAR correspond to hand movement and light perception, respectively.

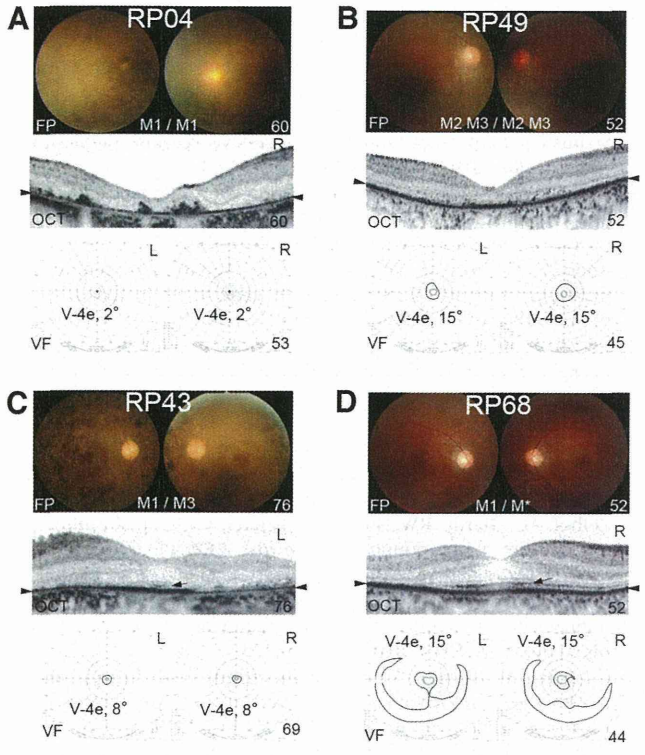

FIGURE 3. Clinical features of patients carrying the truncating mutations. (**A**) RP04 carrying the homozygous p.S1653Kfs*2 mutation (M1). (**B**) RP49 carrying the homozygous p.Y2935* mutation (M2) and the homozygous p.G843E mutation (M3). (**C**) RP43 carrying the heterozygous p.S1653Kfs*2 mutation (M1) and p.G843E mutation (M3). (**D**) RP68 carrying the heterozygous p.S1653Kfs*2 mutation (M1) and unknown mutation (M*). FP, fundus photograph; OCT, optical coherence tomography; VF, visual field; L, left; R, right. The *number* in each panel indicates the age of the patient when the examination was performed. In the OCT panel, an *arrow* indicates the junction between the inner and outer segments of photoreceptors, and an *arrowhead* indicates an RPE complex.

There are several possibilities: the large deletion of an allele that cannot be detected by direct sequencing[2,4]; a second pathogenic mutation located in the promoter region, the 5′-UTR region, the regulatory element in the intron, an unknown exon, or the 3′-UTR region[13]; a mutation in the second gene involved in the maintenance of photoreceptor cells in association with *EYS*. The second mutation in another allele remains to be sought.

The combination of a truncating mutation and p.G843E is intriguing because c.2528G>A generating p.G843E is one of the SNPs with approximately 1% of minor allele frequency. The glycine at position 843 is not only highly conserved among the EGF domains in the EYS protein, it is evolutionarily conserved among EYS homologs from various species (orangutan, marmoset, horse, dog, opossum, platypus, chicken, fly).[13] Thus, p.G843E is possibly pathogenic because of the reduction of EYS function. Alternatively, there may be a p.G843E-linked mutation that causes the reduction of EYS function. If a patient carrying homozygous p.G843E alleles were to be found, the pathogenicity of p.G843E or the p.G843E-linked mutation could be confirmed. RP49 had homozygous p.G843E alleles but also had homozygous p.Y2935* alleles that seem to have been responsible primarily for the manifestation of RP. Because p.Y2935* is located in the EGF domain encoded by the last exon, the transcript may escape degradation by NMD,[23] resulting in the production of a truncated EYS protein lacking the C-terminal EGF and LamG domains. RP49 showed a mild decline in visual acuity compared with the other patients, suggesting that the protein with p.Y2935* and p.G843E may have weak EYS activity. The mild symptoms of patients carrying both p.G843E and a truncation mutation can also be explained by assuming the weak activity of the mutant EYS protein with p.G843E or a reduction of EYS due to the p.G843E-linked mutation. On the other hand, RP50, who carried p.S2428* and p.G843E, completely lost visual acuity, implying that this patient has further mutations in the *EYS* gene or in another gene responsible for maintaining the photoreceptor cells.

Two patients had a single missense change, p.N1163K (c.3489T>A) and p.V1270G (c.3809T>G). p.V1270G is located close to the EGF domain in the N-terminal half region, and a valine at position 1270 is conserved among different species. The pathogenicity of these missense changes remains unclear. p.N1163K concerns a residue in a calcium-binding EGF domain, which is conserved among other EGF domains and among different species. p.N1163K has been reported in two patients of different origins.[9,12] It is possible that these missense changes could be involved in the manifestation of RP in combination with an unknown mutation in another allele.

Although the function of the EYS protein must be completely or almost completely lost in the eyes of patients carrying two alleles with truncating mutations due to degradation of truncated mRNA by NMD or to the loss of the C-terminal region, the patients had normal visual acuity until adolescence, indicating that EYS may be dispensable for the development of photoreceptor cells and that another factor may compensate for the loss of EYS to maintain the function of photoreceptor cells. If this is the case, the severity of symptoms may depend on the amount, activity, or both of this compensating factor. From this perspective, RP12 is interesting because this patient had mild symptoms despite carrying double truncating mutations. This case can be explained by the higher activity of the compensating factor. One candidate for the factor compensating the impaired function of EYS is a variant of EYS. Recently, we showed that human retinoblastoma Y79 expressed three variants of the *EYS* gene, including a long full-length cDNA clone with 7989 bp encoding a short form of EYS with 594 amino acids, but were not able to obtain the full-length cDNA clone encoding the longest form of EYS.[25] Thus, there seem to be many forms of EYS variants, including unknown ones. Given that the short EYS variants contain the N-terminal EGF domains identical to those of the long form, these variants may partially compensate for the loss of the long form of EYS. In addition, the existence of other compensating factors is expected from the fact that *EYS* orthologs are disrupted or absent from rodent genomes.[7]

Eys was first identified as a gene involved in the morphogenesis of the inter-rhabdomere space of *Drosophila* eyes[17,18] and was also shown to be expressed in *Drosophila* mechanosensory organs in which eys provides mechanical support to the mechanoreceptor cell.[26] In the vertebrate, the porcine EYS was shown to localize in the outer segment of the photoreceptor cell layer.[7] These findings lead us to postulate that human EYS may contribute to maintain the structure of the photoreceptor layer by providing rigidity to the outer segment of photoreceptor cells. To understand the disease mechanism caused by mutations observed in the *EYS* gene of arRP patients, it is necessary to reveal the molecular and biochemical characteristics of the EYS protein.

In conclusion, we found that the main cause of nonsyndromic arRP in a Japanese population was mutation in the *EYS* gene and that one-third of the patients with nonsyndromic arRP had founder mutations. In addition, we found that the type of mutation was related to the severity of the symptoms. Thus, genotyping in the *EYS* gene could be a valuable tool for the diagnosis and prediction of the long-term prognosis of

Japanese patients with arRP and thus could be useful for genetic counseling and future gene therapy.

Acknowledgments

The authors thank Akiko Nakajima and Yuuki Noshiro for their technical assistance and all the participating RP patients and control subjects.

References

1. Weleber RG. Retinitis pigmentosa and allied disorders. Ryan SJ ed. *Retina.* 2nd ed. St. Louis: Mosby; 1994:335-466.
2. Nakanishi T, Ishida M, Yanashima K, Neko Y. Results of survey relating to such factors as description and cause of ocular disease of persons with visual impairment who use facilities (Japanese). *Res Bull Natl Rehab Ctr Per Disabilit.* 2006;29:119-127.
3. Rivolta C, Sharon D, DeAngelis MM, Dryja TP. Retinitis pigmentosa and allied diseases: numerous diseases, genes, and inheritance patterns. *Hum Mol Genet.* 2002;11:1219-1227.
4. Hartong DT, Berson EL, Dryja TP. Retinitis pigmentosa. *Lancet.* 2006;368:1795-1809.
5. Klevering BJ, Yzer S, Rohrschneider K, et al. Microarray-based mutation analysis of the ABCA4 (ABCR) gene in autosomal recessive cone-rod dystrophy and retinitis pigmentosa. *Eur J Hum Genet.* 2004;12:1024-1032.
6. Rivolta C, Sweklo EA, Berson EL, Dryja TP. Missense mutation in the USH2A gene: association with recessive retinitis pigmentosa without hearing loss. *Am J Hum Genet.* 2000;66:1975-1978.
7. Abd El-Aziz MM, Barragan I, O'Driscoll CA, et al. EYS, encoding an ortholog of *Drosophila* spacemaker, is mutated in autosomal recessive retinitis pigmentosa. *Nat Genet.* 2008;40:1285-1287.
8. Collin RW, Littink KW, Klevering BJ, et al. Identification of a 2 Mb human ortholog of *Drosophila* eyes shut/spacemaker that is mutated in patients with retinitis pigmentosa. *Am J Hum Genet.* 2008;83:594-603.
9. Audo I, Sahel JA, Mohand-Saïd S, et al. EYS is a major gene for rod-cone dystrophies in France. *Hum Mutat.* 2010;31:E1406-1435.
10. Abd El-Aziz MM, O'Driscoll CA, Kaye RS, et al. Identification of novel mutations in the ortholog of *Drosophila* eyes shut gene (EYS) causing autosomal recessive retinitis pigmentosa. *Invest Ophthalmol Vis Sci.* 2010;51:4266-4272.
11. Bandah-Rozenfeld D, Littink KW, Ben-Yosef T, et al. Novel null mutations in the EYS gene are a frequent cause of autosomal recessive retinitis pigmentosa in the Israeli population. *Invest Ophthalmol Vis Sci.* 2010;51:4387-4394.
12. Littink KW, van den Born LI, Koenekoop RK, et al. Mutations in the EYS gene account for approximately 5% of autosomal recessive retinitis pigmentosa and cause a fairly homogeneous phenotype. *Ophthalmology.* 2010;117:2026-2033.
13. Barragán I, Borrego S, Pieras JI, et al. Mutation spectrum of EYS in Spanish patients with autosomal recessive retinitis pigmentosa. *Hum Mutat.* 2010;31:E1772-E1800.
14. Fukui T, Yamamoto S, Nakano K, et al. ABCA4 gene mutations in Japanese patients with Stargardt disease and retinitis pigmentosa. *Invest Ophthalmol Vis Sci.* 2002;43:2819-2824.
15. Ando Y, Ohmori M, Ohtake H, et al. Mutation screening and haplotype analysis of the rhodopsin gene locus in Japanese patients with retinitis pigmentosa. *Mol Vis.* 2007;13:1038-1044.
16. Jin ZB, Mandai M, Yokota T, et al. Identifying pathogenic genetic background of simplex or multiplex retinitis pigmentosa patients: a large scale mutation screening study. *J Med Genet.* 2008;45:465-472.
17. Husain N, Pellikka M, Hong H, et al. The agrin/perlecan-related protein eyes shut is essential for epithelial lumen formation in the *Drosophila* retina. *Dev Cell.* 2006;11:483-493.
18. Zelhof AC, Hardy RW, Becker A, Zuker CS. Transforming the architecture of compound eyes. *Nature.* 2006;443:696-699.
19. Khan MI, Collin RW, Arimadyo K, et al. Missense mutations at homologous positions in the fourth and fifth laminin A G-like domains of eyes shut homolog cause autosomal recessive retinitis pigmentosa. *Mol Vis.* 2010;16:2753-2759.
20. Oshikawa M, Usami R, Kato S. Characterization of the arylsulfatase I (ARSI) gene preferentially expressed in the human retinal pigment epithelium cell line ARPE-19. *Mol Vis.* 2009;15:482-494.
21. Clark AG. Inference of haplotypes from PCR-amplified samples of diploid populations. *Mol Biol Evol.* 1990;7:111-122.
22. Excoffier L, Slatkin M. Maximum-likelihood estimation of molecular haplotype frequencies in a diploid population. *Mol Biol Evol.* 1995;12:921-927.
23. Holbrook JA, Neu-Yilik G, Hentze MW, Kulozik AE. Nonsense-mediated decay approaches the clinic. *Nat Genet.* 2004;36:801-808.
24. Pieras JI, Barragán I, Borrego S, et al. Copy-number variations in EYS: a significant event in the appearance of arRP. *Invest Ophthalmol Vis Sci.* 2011;52:5625-5631.
25. Oshikawa M, Tsutsui C, Ikegami T, et al. Full-length transcriptome analysis of human retina-derived cell lines ARPE-19 and Y79 using the vector-capping method. *Invest Ophthalmol Vis Sci.* 2011;52:6662-6670.
26. Cook B, Hardy RW, McConnaughey WB, Zuker CS. Preserving cell shape under environmental stress. *Nature.* 2008;452:361-364.

OPEN ACCESS Freely available online

PLoS one

Derivation of Human Differential Photoreceptor-like Cells from the Iris by Defined Combinations of *CRX*, *RX* and *NEUROD*

Yuko Seko[1,2], Noriyuki Azuma[3], Makoto Kaneda[4], Kei Nakatani[5], Yoshitaka Miyagawa[2], Yuuki Noshiro[2], Reiko Kurokawa[1], Hideyuki Okano[4], Akihiro Umezawa[1]*

1 Department of Reproductive Biology, Center for Regenerative Medicine, National Institute for Child Health and Development, Okura, Setagaya, Japan, **2** Sensory Functions Section, Research Institute, National Rehabilitation Center for Persons with Disabilities, Tokorozawa, Japan, **3** Department of Ophthalmology, National Center for Child Health and Development, Setagaya, Japan, **4** Department of Physiology, Keio University School of Medicine, Shinanomachi, Japan, **5** Institute of Biological Science, Tsukuba University, Ten-noudai, Japan

Abstract

Examples of direct differentiation by defined transcription factors have been provided for beta-cells, cardiomyocytes and neurons. In the human visual system, there are four kinds of photoreceptors in the retina. Neural retina and iris-pigmented epithelium (IPE) share a common developmental origin, leading us to test whether human iris cells could differentiate to retinal neurons. We here define the transcription factor combinations that can determine human photoreceptor cell fate. Expression of rhodopsin, blue opsin and green/red opsin in induced photoreceptor cells were dependent on combinations of transcription factors: A combination of *CRX* and *NEUROD* induced rhodopsin and blue opsin, but did not induce green opsin; a combination of *CRX* and *RX* induced blue opsin and green/red opsin, but did not induce rhodopsin. Phototransduction-related genes as well as opsin genes were up-regulated in those cells. Functional analysis; i.e. patch clamp recordings, clearly revealed that generated photoreceptor cells, induced by *CRX*, *RX* and *NEUROD*, responded to light. The response was an inward current instead of the typical outward current. These data suggest that photosensitive photoreceptor cells can be generated by combinations of transcription factors. The combination of *CRX* and *RX* generate immature photoreceptors: and additional *NEUROD* promotes maturation. These findings contribute substantially to a major advance toward eventual cell-based therapy for retinal degenerative diseases.

Citation: Seko Y, Azuma N, Kaneda M, Nakatani K, Miyagawa Y, et al. (2012) Derivation of Human Differential Photoreceptor-like Cells from the Iris by Defined Combinations of *CRX*, *RX* and *NEUROD*. PLoS ONE 7(4): e35611. doi:10.1371/journal.pone.0035611

Editor: Shu-ichi Okamoto, Sanford-Burnham Medical Research Institute, United States of America

Received August 24, 2011; **Accepted** March 19, 2012; **Published** April 25, 2012

Funding: This work was supported by a Grant-in-aid for the Global COE program from MEXT to Keio University. The funders had no role in study design, data collection and analysis, decision to publish, or preparation of the manuscript. No additional external funding received for this study.

Competing Interests: The authors have declared that no competing interests exist.

* E-mail: umezawa@1985.jukuin.keio.ac.jp

Introduction

The possibility of redirecting cell differentiation by overexpression of genes was suggested by Weintraub with the identification of the "master gene," *MyoD* [1]. The process was thought to involve reversion to a less differentiated state, a kind of de-differentiation, before the new cell type is formed. Another process has since been introduced, the concept of "direct conversion" or "direct reprogramming" without de-differentiation. This process is thought to be direct lineage switching [2] rather than lineage switching back to a branch point and out again in a different direction. "Direct conversion" has been shown in beta-cells, cardiomyocytes and neurons: A specific combination of three transcription factors (Ngn3, Pdx1 and MafA) reprogram differentiated pancreatic exocrine cells in adult mice into cells that closely resemble beta cells [3]; a combination of three factors (Gata4, Tbx5 and Baf60c) induces non-cardiac mesoderm to differentiate directly into contractile cardiomyocytes [4]; and a combination of three factors (Ascl1, Brn2 and Myt1l) converts mouse fibroblasts into functional neurons [5]. In this study, we employed the strategy of "direct reprogramming" to generate retinal photoreceptor cells from human somatic cells.

Several retinal diseases, including retinitis pigmentosa, age-related macular degeneration and cone dystrophy, lead to loss of vision due to loss of photoreceptors and retinal pigment epithelium (RPE). Gene therapy has been implicated for Leber's congenital amaurosis [6]. Another promising therapeutic strategy is to transplant functional photoreceptor cells and retinal pigment epithelial cells. Sheets of human fetal neural retina with retinal pigment epithelium [7] and ES cell-derived photoreceptors [8] have been implicated for use as sources for photoreceptor cells. And human ES cell-derived RPE has recently been implicated to patients with macular degeneration [9]. However, the use of human embryos faces ethical controversies that prevent the widespread applications of human fetal tissues and human ES cells. A way to circumvent these issues is to induce photoreceptor-specific phenotypes by direct reprogramming of somatic cells of the patients. During vertebrate eye development, the inner layer of the optic cup differentiates into the neural retina and iris-pigmented epithelium (IPE). This common developmental origin led us to test whether iris cells could transdifferentiate to retinal

neurons and thus be a candidate source of cells for transplantation. We here define the combinations of transcription factors that induce light responsive photoreceptor-like cells in humans.

Results

Cultivation of iris-derived cells

The iris pieces were cut into smaller pieces and served as explants culture. Cells derived from the iris pieces are designated as "iris cells". Iris pigment epithelial cells (IPE cells) were isolated from iris tissues using dispase and trypsin. Residual iris pieces after removal of IPE were cut into smaller pieces and served as explant culture. Outgrowing cells from the explant cultures were designated as "iris-stromal (IS) cells" (Fig. 1A). Ciliary epithelial cells were isolated from pars plana and pars plicata in the same manner as IPE cells. We then performed Southern blot analysis and nucleotide sequencing to investigate whether the RB gene was deleted or mutated, because some irreversibly de-identified iris-derived cells were from the patients with retinoblastoma. Southern blot analysis revealed that the RB gene was not deleted or rearranged in any of the iris-derived cells examined (Fig. S1). Sequencing analysis revealed that cDNAs of the RB gene did not have deletions or mutations at the nucleotide level.

Cultured iris cells show phenotypes of retinal glia and progenitor

Iris cells were immunocytochemically positive for glial cell- and neural stem cell-markers (Fig. 1A, 1B). RT-PCR analysis revealed that these cells expressed markers for glial cells and neural stem cells, indicating that the iris has common features with the retinal glia (Fig. 1C). After neural induction with the B27 medium, rhodopsin was not induced (Fig. 1C). After retinal induction with the R1 medium, green/red opsin was up-regulated significantly but blue opsin and rhodopsin were not up-regulated (Fig. 1D).

Iris cells are induced into a rod- or cone-specific phenotype by defined transcription factors

We selected six genes, *SIX3*, *PAX6*, *RX*, *CRX*, *NRL*, and *NEUROD*, as candidate factors that may contribute to induce photoreceptor-specific phenotypes in iris cells, on the basis that such factors play pivotal roles in the development of photoreceptors. Iris cells were transfected with these genes and were examined for inducible expression of photoreceptor-specific genes in those cells. Transduction of a single gene for *SIX3*, *PAX6*, *RX*, *CRX*, *NRL*, or *NEUROD* induced neither rod- nor cone-specific phenotypes in iris cells, but the six genes together up-regulated blue opsin and rhodopsin (Fig. S2). To determine which of the six candidates were critical, we tested the effect of withdrawal of individual factors from the pool of transduced candidate genes on expression of the opsin genes. We identified two genes, *NEUROD* and *CRX*, which were essential for photoreceptor induction; individual withdrawal of *NEUROD* resulted in loss of expression of rhodopsin and withdrawal of *CRX* resulted in loss of blue opsin.

Then, we tested the combination of only two genes, CRX and NEUROD (Fig. 2A, 2B). The combination of *CRX* and *NEUROD* induced rod photoreceptor specific genes including rhodopsin and other phototransduction genes. After transduction of *CRX* and *NEUROD*, immunostaining showed that 38% of total cells were rhodopsin-positive cells (3,750 cells) (Fig. 2C, Fig. S3). However, this combination did not induce the red opsin gene. Addition of *RX* to the combination of *CRX* and *NEUROD* augmented blue opsin expression (Fig. 2B). After transduction with *CRX*, *RX* and *NEUROD*, rhodopsin-positive, blue opsin-positive and green/red opsin-positive cells were 29% (per 954 cells), 37% (per 235 cells) and 25% (per 193 cells) of total cells, respectively, by immunostaining. Hybrid photoreceptor cells were also detected by double-staining immunocytochemistry (Fig. S4). We then investigated combinations of transcription factors that induce specific types of photoreceptor cells. A combinational approach showed that combination of *CRX* and *RX* was sufficient to induce green/red opsin and other cone-specific genes (Fig. 2D, Fig. S2). *PAX6*(+5a) did not influence cone-related gene induction (Fig. 2E). Expression levels of rhodopsin and blue opsin reached a maximum level by one week after gene transduction and remained unchanged up to 3 weeks. Expression of green/red opsin reached a maximum level 3 days after gene transduction (Fig. 2F). Expression levels of opsin- and phototransduction-related genes were quantitated (Fig. 2G). *NEUROD* significantly decreased expression of the cone-specific genes, i.e. genes for green opsin and cone channel B3 (CNGB3) in human iris cells ($p<0.005$). On the other hand, it was clearly demonstrated that expression of rhodopsin and S-antigen, which are specifically expressed in rod photoreceptors, were much higher in *CRX*, *RX* and *NEUROD*-infected cells than in *CRX* and *RX*-infected cells (rhodopsin, $p<0.05$; S-antigen, $p<0.005$, Welch's t-test). Ultrastructural analysis revealed a cilia-associated structure, i.e. centriole, surrounded by mitochondria (Fig. S5).

Inhibition of factors by small interfering RNA (siRNA)

We performed RT-PCR to investigate if the transgenes continued to be expressed in the generated retinal cells (Fig. 2H, Table S1). The exogenous factors (transgenes) were clearly detected in induced retinal cells. Interestingly, the corresponding endogenous genes intiated expression in the induced retinal cells, similar to what is found in iPS cells. We then suppressed the *CRX* and *NEUROD* genes by siRNA (Fig. S6) to investigate the involvement of the genes in photoreceptor differentiation. Expression of the photoreceptor-specific/associated genes (blue opsin, s-antigen and recoverin) decreased significantly in siCRX and siNEUROD-transfected cells, compared to cells treated with control siRNA, suggesting that CRX and NEUROD are necessary for photoreceptor conversion.

Derivation of photoreceptor-like cells from IPE and IS cells

To investigate photoreceptor cell differentiation from other cell types, we isolated IPE and IS cells from iris tissues. Both cell types began to express opsin genes after transduction of *CRX*, *RX* and *NEUROD* genes (Fig. 3A, 3B). To determine if IPE and IS cells originated from neural ectoderm and neural crest cells, we investigated expression of neural crest marker genes. IPE and IS expressed these neural crest markers at high levels (Fig. 3C). These findings indicate that IS cells derived from neural crest cells, as well as IPE cells, could differentiate into photoreceptor-like cells. We also isolated ciliary epithelial cells from pars plicata and pars plana (Fig. 1A, 3D). Ciliary epithelial cells from pars plicata expressed rhodopsin, blue opsin, and green/red opsin at a high level after transduction with three genes (*CRX*, *RX* and *NEUROD*) or all six genes together (Fig. 3E). Retina-derived Müller glial cells expressed opsin genes after transduction of all genes (Fig. 3F).

Induced photoreceptor-like cells are photoresponsive in vitro

Light stimulation was applied to *CRX*, *RX* and *NEUROD*-infected human iris-derived cells because these infected cells showed the most photoreceptor-like phenotypes by RT-PCR and immunocytochemistry. Both blue and green light stimulation produced inward current (Fig. 4A, 4B). Inward current continued

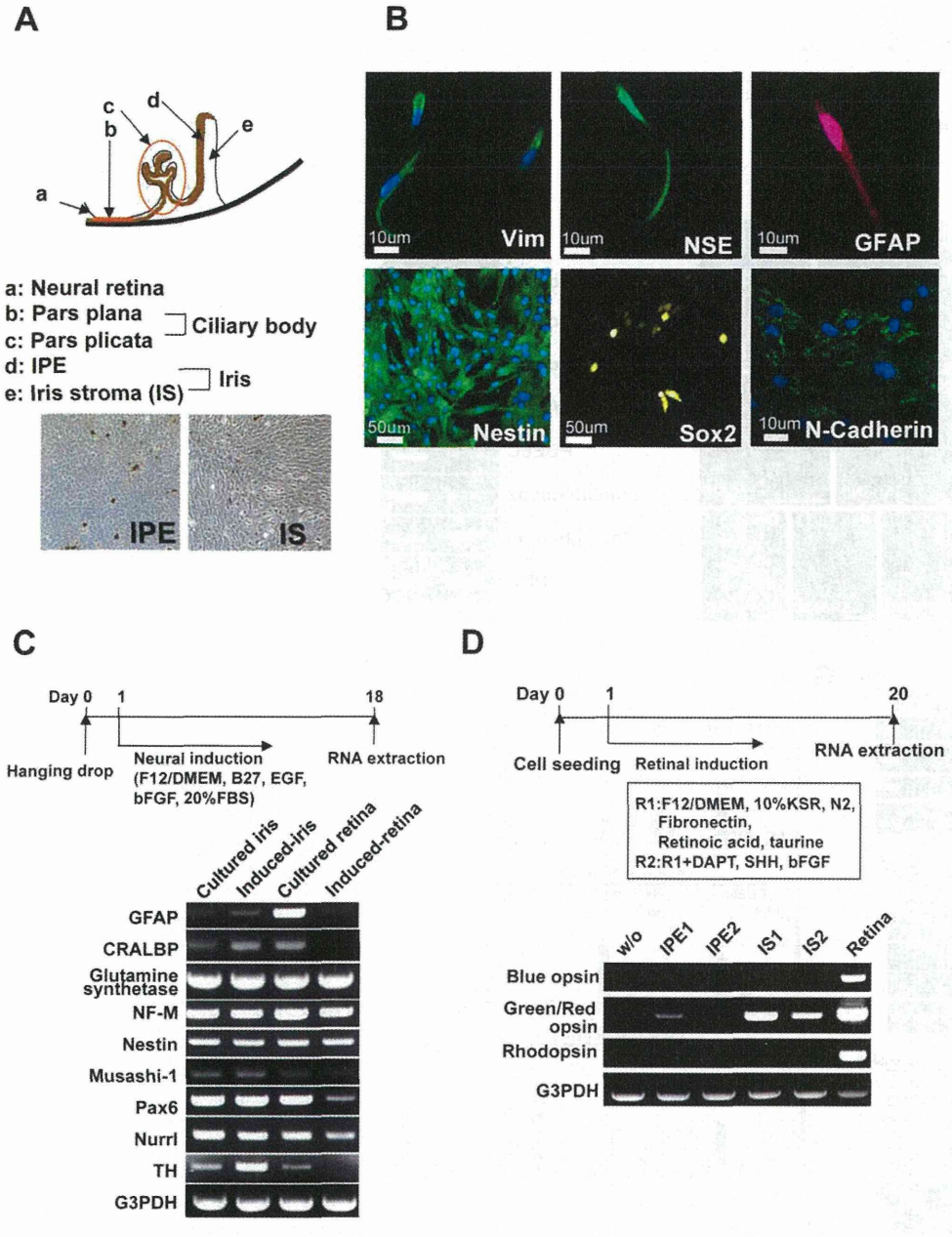

Figure 1. Retinal glia- and retinal progenitor-like phenotypes in iris cells. (A) Scheme of cell sources in the iris and ciliary body. (B) Immunocytochemical analysis of iris cells. Iris cells are immunocytochemically positive for glial cell marker (GFAP), and neural stem cell markers (Nestin (green), Sox2 (yellow) and N-Cadherin (green)). Nuclei were stained with DAPI (blue) with vimentin, nestin and N-cadherin. (C) Expression of neuron-related genes after neural induction. RT-PCR analysis indicates that iris cells expressed glial cell markers (GFAP, CRALBP and glutamine synthetase), and neural stem cell markers (Nestin, Musashi-1 and Pax6). By the "hanging-drop" method coupled with the B27 medium, rhodopsin was not induced. In this illustration, "Induced" indicates "cells at an induced state by the hanging-drop method coupled with the B27 medium" and "Retina" indicates retina-derived cells at passage 3. (D) Expression of the opsin genes after retinal induction. In this illustration, "w/o" indicates iris-stromal cells without any induction. "IPE" and "IS" indicate "iris pigment epithelial cells" and "iris-stromal cells", respectively, that were induced by exogeneously added chemicals and growth factors as indicated. By retinal induction with the R1 medium, green/red opsin was up-regulated significantly in iris-stromal cells, but blue opsin or rhodopsin was not up-regulated.
doi:10.1371/journal.pone.0035611.g001

to flow after the offset of light stimulation but only four cells showed partial or complete recovery within 60 sec after the cessation of light stimuli (n = 9), presumably reflecting the limited expression or absence of inactivation machinery. Inward current to blue light stimulation was observed in three out of four cells and inward current to green light stimulation was observed in six out of six cells. Light stimulation to non-infected control cells (blue, n = 2; green, n = 2) did not produce any inward current. These results indicate that the combination of *CRX*, *RX* and *NEUROD* transforms human iris-derived cells into photoresponsive photoreceptor-like cells in vitro, although the typical outward current of photoreceptor cells could not be detected. Since the light-induced inward current seemed to be mediated by melanopsin-associated phototransduction, we investigated expression of melanopsin by

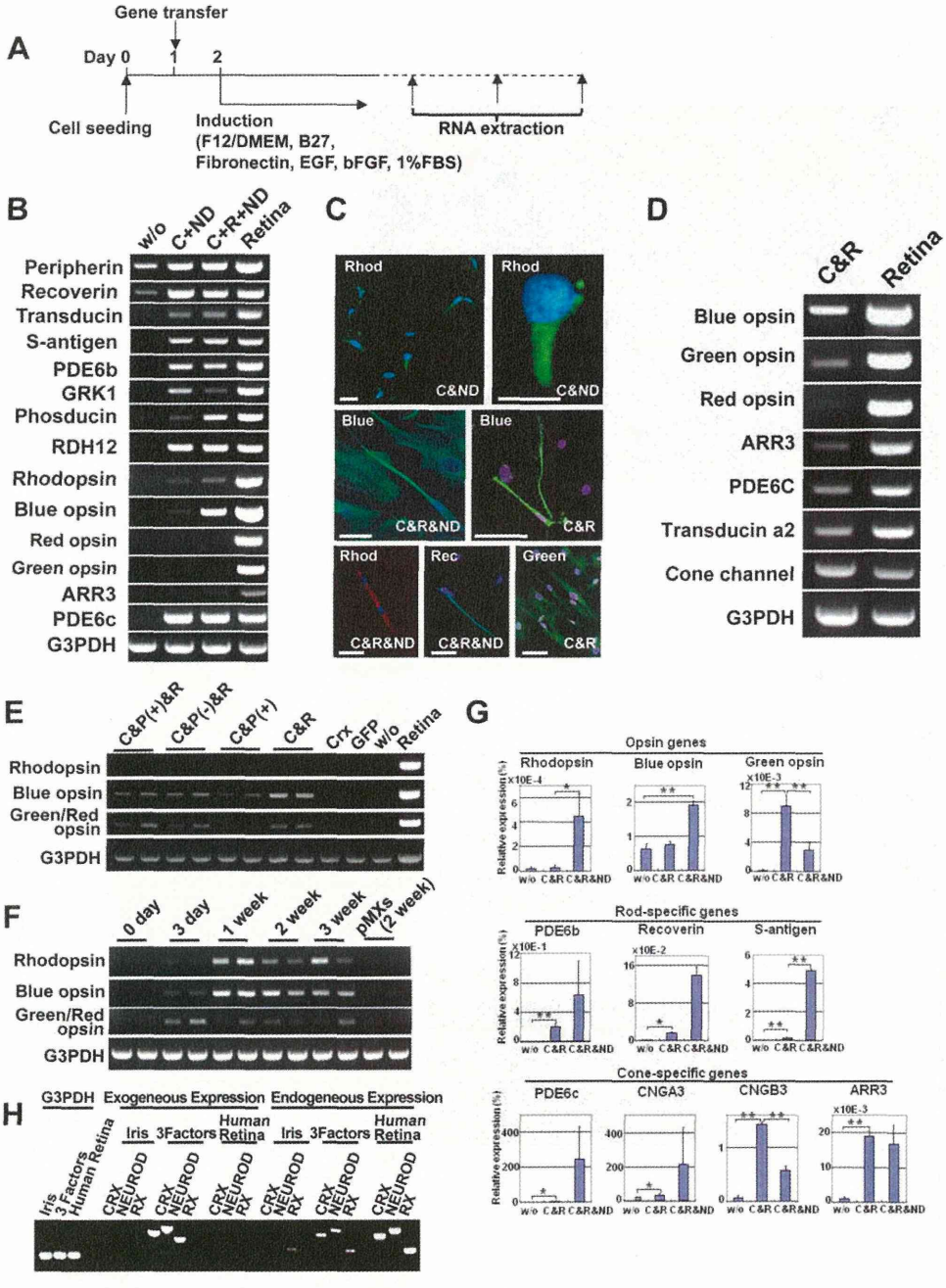

Figure 2. Induction of rod- or cone-specific phenotypes in human iris cells by the defined transcription factors. (A) Protocol to induce rod- or cone-specific phenotypes in human iris cells by the defined transcription factors. (B) Expression of rod-specific genes in iris cells after transduction of the combination of *CRX* and *NEUROD* or the combination of *CRX*, *RX*, and *NEUROD*. The combination of only two genes, *CRX* and *NEUROD* induced expression of rhodopsin, i.e. rod-photoreceptor specific opsin. Addition of *RX* to *CRX* and *NEUROD* enhanced blue opsin expression. "w/o": cultured iris-derived cells without gene transfer as a negative control; "Retina": human retinal tissue as a positive control. (C) Immunocytochemistry using antibodies to blue opsin (green), green/red opsin (green), rhodopsin (green or red) and recoverin (green). Nuclei were stained with DAPI (blue). Experiments were performed at two weeks after infection. "Blue": blue opsin; "Green": green/red opsin; "Rhod": rhodopsin; "Rec": recoverin. Scale bars represent 10 μm in the upper left panel and 50 μm in the other panels. (D) Transduction of cone-specific genes in iris cells. Cone-specific phenotypes were induced by the transcription factors, i.e., the combination of *CRX* and *RX*. The combination of *CRX* and *RX* induced other cone-specific genes in addition to the blue opsin, green opsin and red opsin genes. (E) Effect of *PAX6* (+5a) on expression of opsin genes. "Retina": human retinal tissue as a positive control; "w/o": cultured iris-derived cells without gene transfer as a negative control; "GFP": cultured iris-derived cells after transduction of GFP genes as another negative control. (F) Time course of gene expression after transduction of *RX*, *CRX* and *NEUROD*. Expression of the rhodopsin and blue opsin genes increased one week after transduction and then remained unchanged at a later stage. Expression of the green/red opsin gene reached a maximum level three days after infection. Each independent experiment was performed in duplicate as shown in the panel. (G) Quantitative RT-PCR results for rhodopsin, blue opsin, green opsin, PDE6b, recoverin, S-antigen, PDE6c, cone channel A3, cone channel B3 and arrestin3 (ARR3). Vertical axis indicates expression levels of each gene (%) in the indicated cells, relative to human retinal tissues. *$p<0.05$ and **$p<0.005$ (Welch's t-test). (H) RT-PCR analysis of the exogenous and endogenous genes in induced retinal cells. Expression of the *CRX*, *NEUROD* and *RX* genes in the iris cells and transgene-induced cells was analyzed by RT-PCR, using the exogenous and endogenous gene-specific primers (Table S1). Human retina served a control for the endogenous genes. Equal amounts of RNAs were examined by expression of the G3PDH gene.

doi:10.1371/journal.pone.0035611.g002

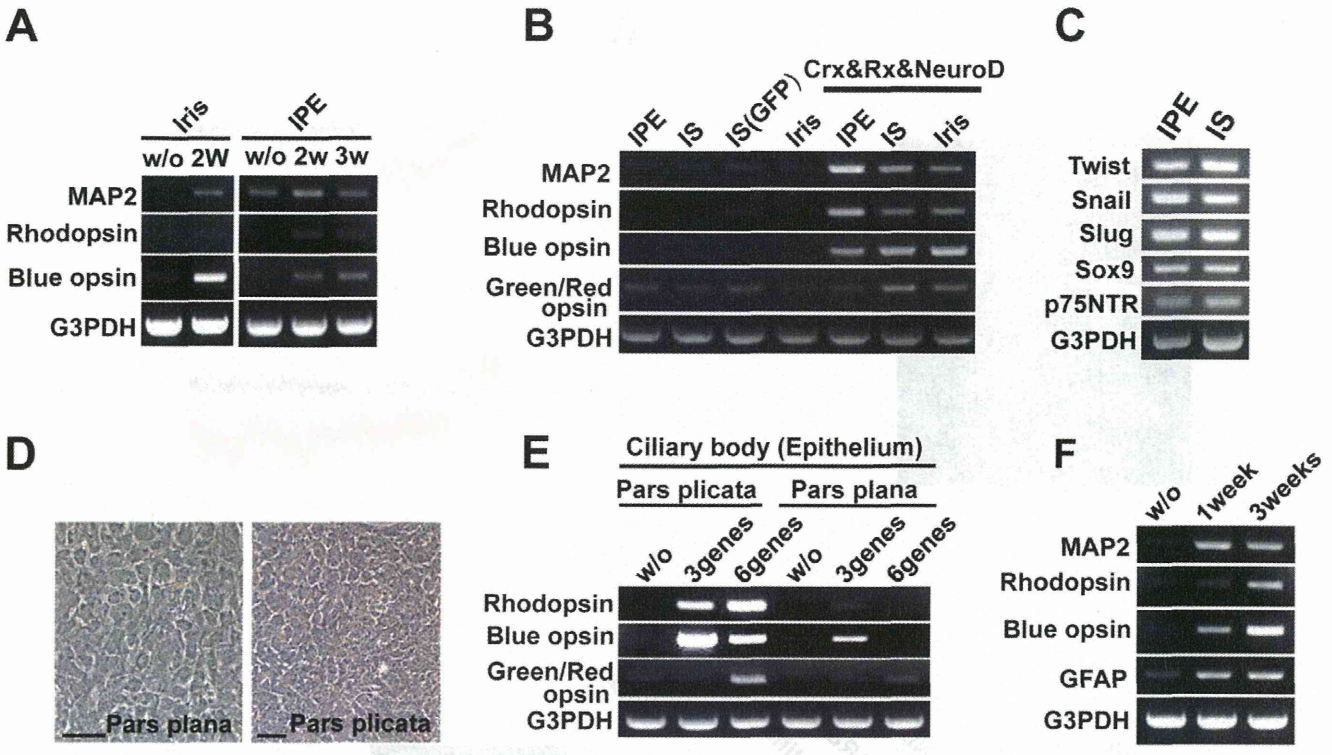

Figure 3. Induction of opsin genes in human iris-derived cells, ciliary epithelial cells and retina-derived cells by the retroviral infection of all the 6 genes and genes for *RX, CRX* and *NEUROD*. (A) RT-PCR analysis for genes of MAP2, rhodopsin, blue opsin and G3PDH in two kinds of iris cells after gene transfer of all the six genes. All six genes were infected into two kinds of iris cells: IPE and stromal cells derived from the peripheral iris, and purely isolated IPE cells. In both cell types, rhodopsin and blue opsin genes were up-regulated. "w/o": cultured iris-derived cells without gene transfer as a negative control. (B) Expression of the rhodopsin and blue opsin genes started two weeks after infection. "IS", "IPE" and "Iris (central)" indicate "iris-stromal cells", "iris pigment epithelial cells", and "central iris cells", respectively. "IS (GFP)" is "iris-stromal cells infected with the GFP gene". In all kinds of iris cells, transduction of the three genes, that are *RX, CRX* and *NEUROD*, enhanced expression of rhodopsin, blue opsin and green/red opsin. (C) RT-PCR analysis for genes for genes of neural crest-related markers in two kinds of iris-derived cells: iris stromal cells and iris pigmented epithelial cells. (D) Phase-contrast photomicrograph of ciliary epithelial cells from pars plana (left) and pars plicata (right). (E) RT-PCR analysis for genes of rhodopsin, blue opsin, green/red opsin and G3PDH in human ciliary epithelium (pars plicata and pars plana) after gene transfer of either all the six genes (*SIX3, PAX6, RX, CRX, NEUROD, NRL*) or three genes (*CRX, RX* and *NEUROD*). (F) RT-PCR analysis for the MAP2, rhodopsin, blue opsin, GFAP and G3PDH genes in retina-derived cells after transfer of all six genes. "w/o": Retina-derived cells without gene transfer 21 days after the start of cultivation. Genes for MAP2, rhodopsin, and blue opsin started to be expressed after the gene transfer.
doi:10.1371/journal.pone.0035611.g003

RT-PCR and immunocytochemistry. *CRX*, *RX* and *NEUROD*-infected iris-derived cells expressed melanopsin (Fig. 4C, 4D), suggesting a larger contribution of melanopsin-associated inward current.

Discussion

This is the first report that functional photosensitive photoreceptor-like cells can be induced from human somatic cells. The present study shows that rod- and cone-photoreceptor-specific phenotypes were induced by transduction of a combination of *CRX*, *RX* and *NEUROD* genes, and that those cells responded to light electrophysiologically. In the retina, rod- and cone-photoreceptors convert light information to electrical signals that are relayed to the brain through several interneurons. In the present study, a combination of *CRX*, *RX* and *NEUROD* induced all of the opsin genes: blue opsin, green/red opsin and rhodopsin (Table S2). On the other hand, a combination of *CRX* and *RX* induced only cone-specific opsin, and additional transduction of *NEUROD* up-regulated rod-specific opsin and rod-specific phototransduction related genes.

Rod photoreceptor generation from iris cells required *NEUROD* in our study. NeuroD is a regulator of both rod photoreceptors [10,11] and cone photoreceptors [12] during mouse development. NeuroD overexpression increases amacrine cells and rod photoreceptors, reduces bipolar cells, and inhibits formation of Müller glia. It has been known since the early 1960s that there is a defined sequence in formation of retinal neurons, which is largely conserved across vertebrates: Cone photoreceptors are generated during early stages of development, and most rod photoreceptors are generated in the latter half of the period of retinogenesis [13]. Similarly, cone photoreceptors are generated at the early stages during ES cell differentiation and rod photoreceptors are generated at a later stage. The present study and these previous reports suggest that NeuroD may work downstream to regulate the development of rod-photoreceptors. NeuroD generally functions in a cell cycle-specific manner, and promotes cell cycle exit [11]. Rod formation may thus be mediated via cessation of cell cycle by NeuroD at the later stage.

It has been hypothesized that retinal stem cells can be found in the ciliary body [14], postnatal retina, and the iris [15]. Pure populations of IPE cells isolated from rat and chicken irises were shown to demonstrate "stemness" [16]. A portion of purely isolated IPE cells of rodents, especially nestin-positive IPE cells, differentiated into multiple neuronal cell types, pan-neural marker- expressing cell types and retina-specific cell types without

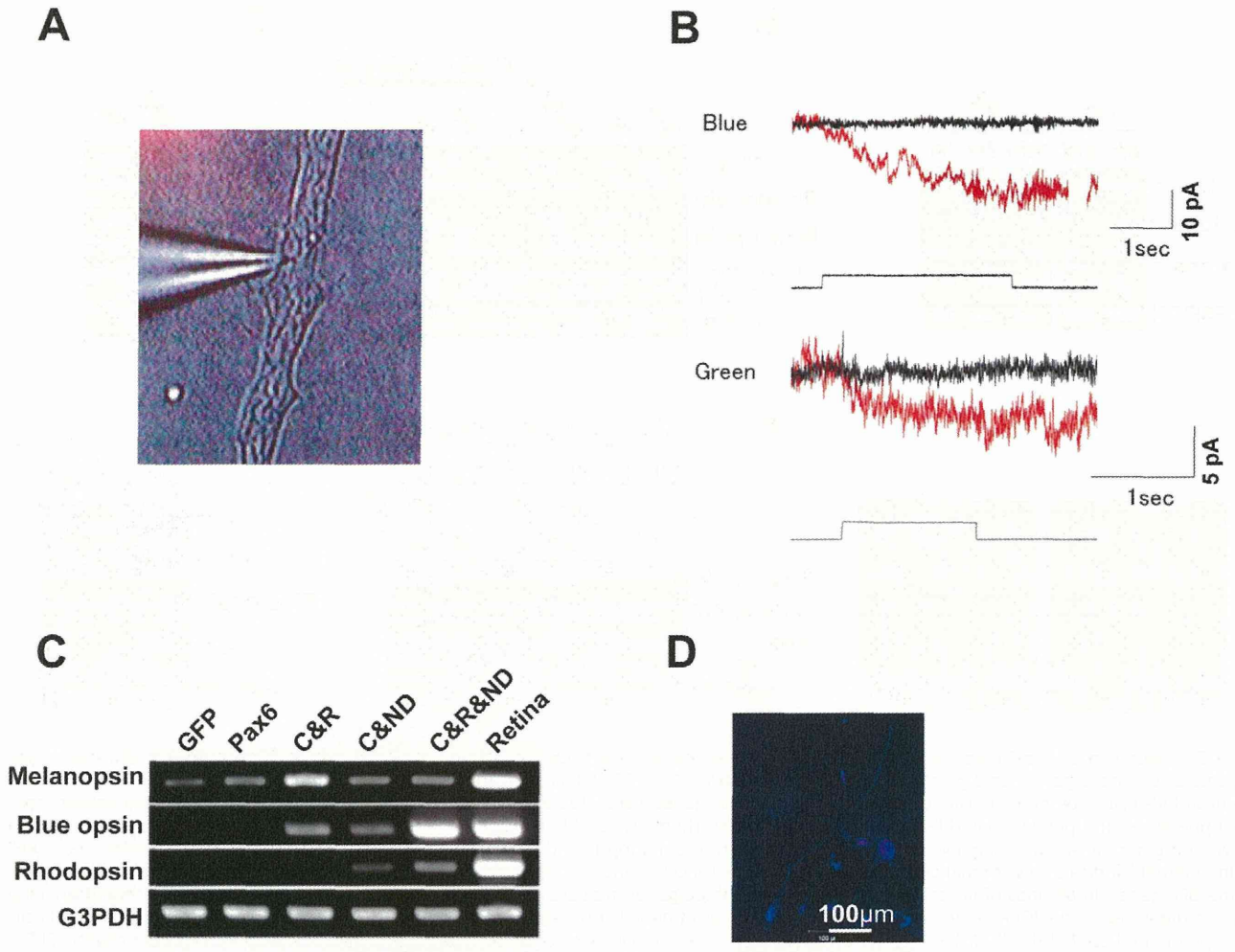

Figure 4. Electrophysiological analysis of the induced photoreceptor-like cells. (A) Recording electrode patched onto infected cells. (B) Responses to blue light (upper panels) or green light (lower panels) in infected cells (red) and non-infected cells (black). The light onset for transfected cells and non-transfected cells had the same timing. The square under the current trace is a timing and duration of light stimulation for transfected cells. The longer light stimulation was given to non-infected cells to rule out any possible artifact. Holding potential was −40 mV. Larger baseline noise in the infected cells probably reflects the channel activities. (C) RT-PCR analysis for genes of melanopsin, rhodopsin, blue opsin and G3PDH in iris cells after gene transfer. Cells were infected with retroviruses carrying the genes for GFP, *PAX6* (+5a) (Pax6), *CRX* & *RX* (C&R), *CRX* & *NEUROD* (C&ND) and *CRX* & *RX* & *NEUROD* (C&R&ND). "Human retina": human retinal tissue, as a positive control. (D) Immunocytochemistry for melanopsin in iris-derived cells after transduction of *CRX, RX* and *NEUROD*. Nuclei were stained with DAPI (blue).
doi:10.1371/journal.pone.0035611.g004

genetic manipulation. On the other hand, it has been shown that retinal stem cells are not present in the human iris [17,18]. The present study demonstrates that human iris cells expressed stem cell markers such as nestin, N-cadherin, Sox2, Musashi-1 and Pax6. Expression of stem cell markers in iris cells may be attributed to the cell source, i.e. cells from infants. However, photoreceptor cell differentiation with exogenously added chemicals and growth factors was limited; that is, only green/red opsin was induced (Fig. 1). Other experimental evidence has also suggested the limitation in mammals without genetic manipulation. Progenitor cells from the mammalian iris, pars plana, and ciliary body do not show a convincing immunoreactivity for rhodopsin, phosducin, recoverin, PKC, or RPE65 [19], but are induced into photoreceptor progeny with retinal transcription factors [20,21]. We first indicate that human IS cells that originate from neural crest (Fig. 3C), as well as IPE cells, differentiate into photoreceptor-like cells. Derivation of photoreceptor-like cells can be attributed to transgene-dependent differentiation of retinal progenitors that exist in the iris.

Our data show that induced photoreceptor-like cells have rod- and cone-signaling-pathways by RT-PCR and immunocytochemistry. In addition, expression of melanopsin was also detected in these cells. Photostimulation of the rod-or cone-pathway produces hyperpolarizing responses, while activation of the melanopsin-pathway produces depolarizing responses [22,23,24,25,26]. Melanopsin is intrinsically expressed in iris cells of the human (Fig. 4C), mouse [27] and Xenopus [24]. Melanopsin signaling has recently been reported to exist in both the iris and retina in mammals [27]. However, photostimulation did not produce any response in non-transfected human iris cells, suggesting the absence of phototransduction machineries *per se*. The light-induced depolarizing responses in infected cells indicate that phototransduction machinery for melanopsin-pathway was induced in infected cells. This is different from the results of infected monkey and rodent iris cells, where photostimulation produced hyperpolarizing responses

[20]. Our data demonstrate that transduction of three transcriptional factors strongly induces expression of blue opsin, which suggests a potential to produce hyperpolarizing responses. One plausible reason for the differences is that numbers of expressed phototransduction machineries for rod-or cone-pathways are not enough in those cells, e.g. outer segments were not observed at an ultrastructural level. Although the reason for depolarization in transfected cells cannot be fully explained so far, it is likely that melanopsin-associated photoresponses may overcome cone- or rod- mediated photoresponses.

In addition to revealing insights into retinal transdifferentiation, this study describes the development of a novel experimental approach to genetic retinal diseases that may be relevant for beta cells, cardiomyocytes, and neurons [3,4,5]. Optimal donor cells for retinal transplantation are post-mitotic photoreceptor precursors but not mature photoreceptors [28]. Immature photoreceptors generated from ES cells or iPS cells in vitro differentiate through transplantation into the mouse retina [29,30]. In this aspect, the induced retinal cells shown here may be suitable for future cell-based therapy since they are not fully differentiated. Together, the finding contributes substantially to an advance toward cell-based therapy for retinal genetic diseases.

Materials and Methods

Preparation of tissue and cell culture

Cells were obtained from donors at ages of 10 months, 1 year 8 months and 3 years. Iris tissues were excised from surgical specimens as a therapy for retinoblastoma with the approval of the Ethics Committee of the National Institute for Child and Health Development (NCCHD), Tokyo. The ethics committee of the NCCHD specifically approved this study (approval number, #156). Signed informed consent was obtained from the parents of the donors, and the surgical specimens were irreversibly de-identified. All experiments handling human cells and tissues were performed in line with the Tenets of the Declaration of Helsinki.

The iris was freed from the ciliary body. The iris kept away from a tumor and invasion of retinoblastoma cells were not detected by a pathologist's examination. The iris pieces were cut into smaller pieces and were subjected to explant-culture in the growth medium [Dulbecco's modified Eagle's medium (DMEM)/Nutrient mixture F12 (1:1) supplemented with 10% fetal bovine serum, insulin-transferrin-selenium, and MEM-NEAA (GIBCO)]. Cells derived from the iris pieces were designated as "iris cells". "IPE cells" were isolated from iris tissues using dispase and trypsin. "Iris cells" without "IPE cells" were designated as "iris-stromal (IS) cells" (Fig. 1A). Ciliary epithelial cells were isolated from pars plana and pars plicata in the same manner as IPE cells. Retinal pieces were cut into smaller pieces and were subjected to explant-culture in the same growth medium as iris cells. Second-passage cells were used for all the experiments.

Sequencing of the RB gene

Total RNA was isolated from iris-derived cells of the three donors used in this study. An aliquot of total RNA was reverse transcribed into cDNA. The full-length of RB gene was amplified with Go-Taq polymerase (Promega) using the cDNA. Direct sequencing was performed with a BigDye® Terminator Cycle Sequencing Kit (Applied Biosystems, Foster City, CA). Sequencing reaction products were run on an automated capillary sequencer (Applied Biosystems 3130xl Genetic Analyzer; Applied Biosystems).

Hanging drop method

Droplets, each of which included 1000 cells in 20 µl of culture medium, were formed on the inverted underside of a single Petri dish cover. The inverted bottom was then set on the top and the entire assembled Petri dish was re-inverted to its normal orientation. The drops of cell suspension were then hanging in the interior of the dish from the inner surface of the cover. The dishes were carefully placed into a 37°C incubator in an atmosphere of 5% CO_2. Aggregates of cells were allowed to form in the drops for 24 h. Formed aggregates were then transferred to a Poly-D-lysine/laminin-coated 6-well tissue-culture plate (Becton Dickinson) (4 aggregates per well).

Plasmid construction

Full length of transcription factors *SIX3* [31], *PAX6* [32], *RX* [33], *CRX* [34], *NRL* [35,36] and *NEUROD* [10], were amplified from cDNAs prepared from total RNA of adult human retina (Clontech, CA, USA) by PCR, and cloned into the XmnI-EcoRV sites of pENTR11 (Invitrogen). Each vector contains one transcription factor and a mixture of vectors was used.

Preparation and infection of recombinant retrovirus

The resulting pENTR11-transcription factors were recombined with pMXs-DEST by use of LR recombination reaction as instructed by the manufacturer (Invitrogen). pMXs was a gift from Dr. Kitamura (Tokyo University) and was modified into pMXs-DEST in our laboratory [37]. The retroviral DNAs were then transfected into 293FT cells and three days later the media were collected and concentrated. The iris-derived cells were prepared on laminin-coated six-well dishes or four-well chamber slides and maintained for one day. The cells were infected with above-mentioned media containing retroviral vector particles with 8 µg/ml of polybrene for 5 h at 37°C. After retroviral infection, the media were replaced with the DMEM/F12/B27 medium supplemented with 20 ng/ml bFGF, 40 ng/ml EGF, fibronectin, and 1% FBS. The retrovirus-infected cells were cultured for up to 21 days. We transfected retroviral eGFP under the same conditions to measure efficiency of infection. The frequency of eGFP-positive cells was 90–94% of all cells at 48 h after infection.

Reverse transcriptase-PCR

Total RNA was isolated with an RNeasy Plus mini-kit® (Qiagen, Maryland, USA) or a PicoPure™ RNA Isolation Kit (Arcturus Bioscience, CA, USA) according to the manufacturer's instructions. An aliquot of total RNA was reverse transcribed using an oligo(dT) primer. The design of PCR primer sets is shown in Table 1.

Quantitative RT-PCR

The cDNA templates were amplified (ABI7900HT Sequence Detection System) using the Platinum Quantitative PCR SuperMix-UDG with ROX (11743-100, Invitrogen). Fluorescence was monitored during every PCR cycle at the annealing step. The authenticity and size of the PCR products were confirmed using a melting curve analysis (using software provided by Applied Biosystems) and a gel analysis. mRNA levels were normalized using G3PDH as a housekeeping gene. The design of PCR primer sets is shown in Table 2.

Immunocytochemistry

Immunocytochemical analysis was performed as previously described [38]. As a methodological control, the primary antibody was omitted. The primary and secondary antibodies used were as

Table 1. Primer sequences for RT-PCR.

Gene name	Forward	Reverse
Pax6	5′ – GTAGTTTCAGCACCAGTGTCTACC – 3′	5′ – GGCTGACTGTTCATGTGTGTCT – 3′
Rhodopsin	5′ – CAACTACATCCTGCTCAACCTAGC – 3′	5′ – GTGTAGTAGTCGATTCCACACGAG – 3′
Glutamine synthetase	5′ – GACCCTAACAAGCTGGTGTTATGT – 3′	5′ – ATGTACTTCAGACCATTCTCCTCC – 3′
CRALBP	5′ – GTCCTCTCTAGTCGGGACAAGTATG – 3′	5′ – CTGGTAGAAACCAGAAAGGTCATC – 3′
Recoverin	5′ – AGAGCATCTACGCCAAGTTCTTCC – 3′	5′ – GCAGAATTTCCTTATTGGCCAGTGTC – 3′
Peripherin	5′ – GTACCTGGCTATCTGTGTTCTCTTC – 3′	5′ – GTCGTAACTGTAGTGTGCTGAGTTG – 3′
Blue opsin	5′ – GCGCTACATTGTCATCTGTAAGCC – 3′	5′ – GAAGGAATGGTGACAAGCCGTAAG – 3′
Green/Red	5′ – GTGCAGTCTTACATGATTGTCCTC – 3′	5′ – AGATAACGGGGTTGTAGATAGTGG – 3′
Green	5′ – GTGATGGTCCTGGCATTC – 3′	5′ – GAGGACACAGATGAGACCTCCGTT – 3′
Red	5′ – GTGATGATCTTTGCGTAC – 3′	5′ – GAGGACACAGATGAGACCTCCGTT – 3′
Transducin-α2-chain	5′ – ATTACAGACCCTGAGTACCTCCCTA – 3′	5′ – GAGGTCCTTCTTGTTGAGAAAGAG – 3′
Cone channel A3 (CNGA3)	5′ – GTCCTGTATGTCTTGGATGTGC – 3′	5′ – GAATCAATCTTGGCCTGGAACTCTG – 3′
Transducin	5′ – CATCGAGACGCAGTTCTCCT – 3′	5′ – AGTAGCGGTGGTTGCAGATG – 3′
Phosducin	5′ – TCAAAGGAACGAGTCAGCAG – 3′	5′ – CTGCTGCAAGGCATGTTAAA – 3′
PDE6b	5′ – CAGTGATGAACACCGACACC – 3′	5′ – ATTTGACCAGGTCCAGTTCG – 3′
PDE6c	5′ – CTGAGGTGGCCTCTAGGTTG – 3′	5′ – GCTGGTGTGATGAAGCCTTAG – 3′
Rhodopsin kinase (GRK1)	5′ – GGACTGGTTCCTGGACTTCA – 3′	5′ – AAGCCAGGGTTCTCCTCATT – 3′
S-antigen	5′ – GGTGTTGTCCTGGTTGATCC – 3′	5′ – TCAGCGTCTTGGTCAAAGTG – 3′
Arrestin3 (ARR3)	5′ – GGTGTTGTCCTGGTTGATCC – 3′	5′ – GTCACAGAACAGGGCAGGTT – 3′
Retinol dehydrogenase 12 (RDH12)	5′– CTTCTCCCCCTTTGTCAAGA – 3′	5′ – CTTTAGGGTTGGCCTTCTCC – 3′
GFAP	5′– GATCAACTCACCGCCAACAG – 3′	5′ – GGACGCCATTGCCTCATACTG – 3′
Nurr1	5′– TTTCTGCCTTCTCCTGCATT – 3′	5′ – GTGGCACCAAGTCTTCCAAT – 3′
Nestin	5′ – AGAGGGGAATTCCTGGAG – 3′	5′ – CTGAGGACCAGGACTCTCTA – 3′
NF-M	5′ – TGAGCTACACGTTGGACTCG – 3′	5′ – TCTCCGCCTCAATCTCCTTA – 3′
Sox-2	5′ – CACAACTCGGAGATCAGCAA – 3′	5′ – GTTCATGTGCGCGTAACTGT – 3′
MAP-2	5′ – GGATTCTGGCAGCAGTTCTC – 3′	5′ – TCCTTGCAGACACCTCCTCT – 3′
Musashi1	5′ – CGAGCTTACAGCCATTCCTC – 3′	5′ – ACTCGTGGTCCTCAGTCAGC – 3′
Tyrosine hydroxylase	5′ – GTCCCGAGCTGTGAAGGTGTTTGA – 3′	5′ – ATTGTCTTCCCGGTAGCCGCTGAA – 3′
Twist	5′ – GTCCGCAGTCTTACGAGGAG – 3′	5′ – GCTTGAGGGTCTGAATCTTGCT – 3′
Snail	5′ – AATCGGAAGCCTAACTACAGCG – 3′	5′ – GTCCCAGATGAGCATTGGCA – 3′
Slug	5′ – AAGCATTTCAACGCCTCCAAA – 3′	5′ – AGGATCTCTGGTTGTGGTATGAC – 3′
Sox9	5′ – AGACAGCCCCCTATCGACTTC – 3′	5′ – TGCTGCTTGGACATCCACAC – 3′
P75NTR	5′ – CCTACGGCTACTACCAGGATG – 3′	5′ – CACACGGTGTTCTGCTTGTC – 3′
Melanopsin	5′ – CTTCACCAGTAGCCTCTATAAGCAG – 3′	5′ – CCCTGAAGATGAAGATGTAGCAGT – 3′
G3PDH	5′ – GCTCAGACACCATGGGGAAGGT – 3′	5′ – GTGGTGCAGGAGGCATTGCTGA – 3′

doi:10.1371/journal.pone.0035611.t001

follows: blue opsin (rabbit polyclonal, H-40, Santa Cruz), green/red opsin (goat polyclonal, C-19, Santa Cruz), rhodopsin (goat polyclonal, I-17, Santa Cruz), N-Cadherin (rabbit polyclonal, Abcam), GFAP (rabbit polyclonal, DAKO), NSE (mouse monoclonal, VI-H14, DAKO), Vimentin (mouse monoclonal, V9, DAKO), Nestin (mouse monoclonal, clone196908, R&D), Sox2 (rabbit polyclonal, ab15830, Abcam), melanopsin (goat polyclonal, C-16, Santa Cruz), recoverin (mouse monoclonal, 6A55CD6, Santa Cruz).

Light stimulation

A high pressure UV lamp (USH-102D, Ushio) was used as a light source. Diffuse, unpolarized blue and green lights were generated through bandpass filters attached with the fluorescent emission system (BX-FLA, Olympus, Tokyo, Japan). Wavelength of light for stimulation was 460–490 nm for blue and 520–550 nm for green. Duration and timing of light stimulation was monitored by a photodiode (TPS708, Toshiba). Light intensity was calibrated by a light meter (LI-COR, LI-250) that was placed at the focal plane on the stage. To maximize a chance for photoisomelization of photopigment, we applied a strong light to the cell. Light intensity used for stimulation was 390 W/m^2 for blue and 4810 W/m^2 for green.

Electrophysiology

To activate the phototransduction cascade, 11-cis retinal (a gift from the vision research community, the National Eye Institute, National Institutes of Health) was added to the culture medium of the human iris-derived cells to a concentration of 50 μM with